

Recent results on proton charge radius and polarizabilities

Haiyan Gao

Duke University & Brookhaven National Laboratory



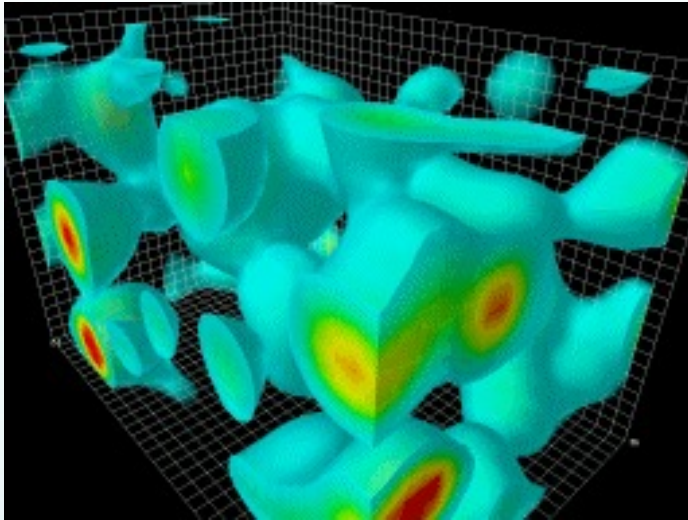
25th European Conference on Few-Body Problems in Physics

July 30, 2023 to August 4, 2023
Alte Mensa
Europe/Berlin timezone

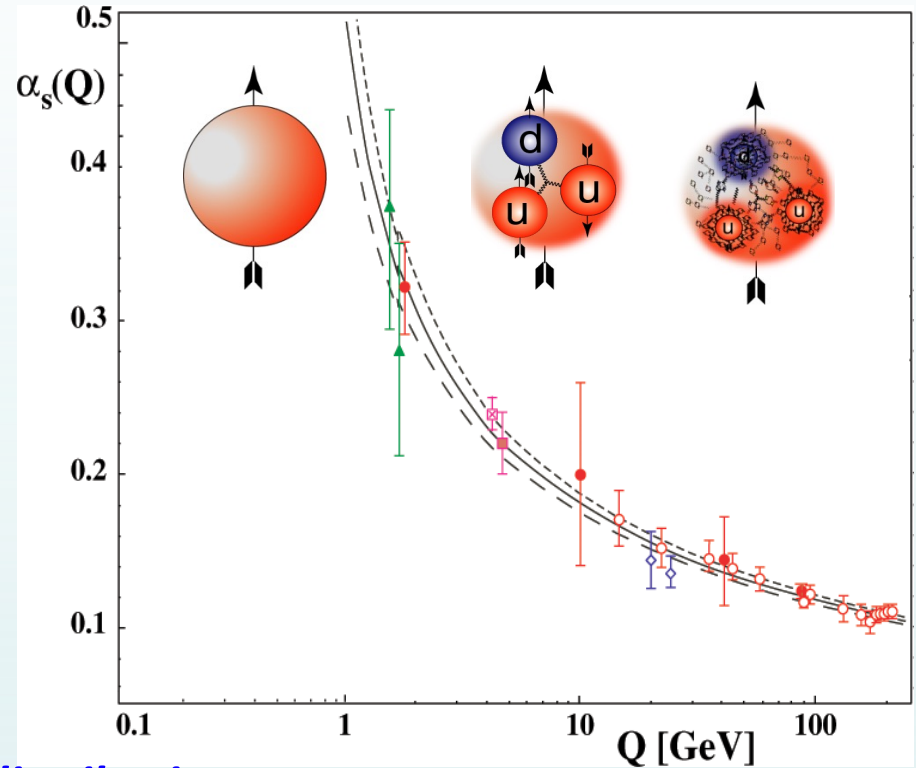
Enter your search term



QCD: still unsolved in non-perturbative region



Credit: D. Leinweber



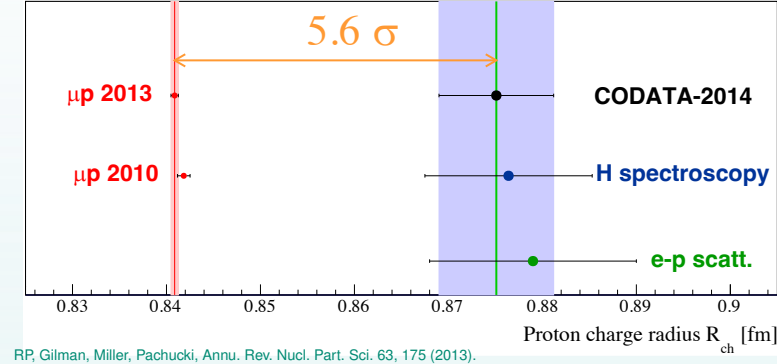
Gauge bosons: gluons

- Charge and magnetism (current) distribution
- Spin and mass decomposition
- Quark momentum and flavor distribution
- Polarizabilities
- Strangeness, charm content
- Three-dimensional structure
- more

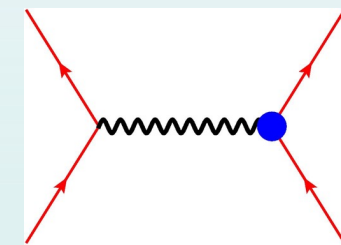
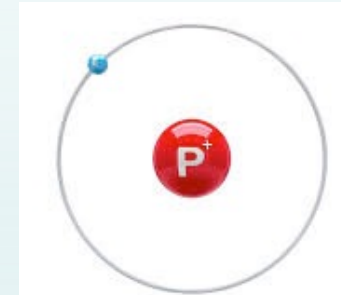
- 2004 Nobel prize for “asymptotic freedom”
- **non-perturbative regime QCD ?????**
- One of the top 10 challenges for physics!
- QCD: Important for discovering new physics beyond SM
- Nucleon structure is one of the most active areas

Proton Charge Radius and the Puzzle

- Proton charge radius:
 - An important quantity for proton
 - Important for understanding how QCD works
 - An important physics input to the bound state QED calculation, affects muonic H Lamb shift ($2S_{1/2} - 2P_{1/2}$) by as much as 2%, and critical in determining the Rydberg constant



- Methods to measure the proton charge radius:
 - Hydrogen spectroscopy (atomic physics)
 - Ordinary hydrogen
 - Muonic hydrogen
 - Lepton-proton elastic scattering (nuclear physics)
 - ep elastic scattering (Mainz-A1, PRad,..)
 - μp elastic scattering (MUSE, AMBER)



- Important point: the proton radius measured in lepton scattering defined the same as in atomic spectroscopy (G.A. Miller, 2019)

$$\begin{aligned} \Delta E &= -4\pi\alpha G_E^{\prime p}(0) |\psi_{n0}(0)|^2 \delta_{l0} \\ &= 4\pi\alpha \frac{r_p^2}{6} |\psi_{n0}(0)|^2 \delta_{l0}. \end{aligned}$$

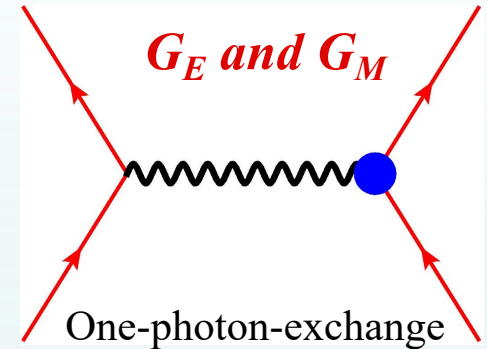
$$\sqrt{\langle r^2 \rangle} = \sqrt{-6 \frac{dG(q^2)}{dq^2} \Big|_{q^2=0}}$$

Electron-proton elastic scattering

- Unpolarized elastic e-p cross section (*Rosenbluth separation*)

$$\frac{d\sigma}{d\Omega} = \frac{\alpha^2 \cos^2 \frac{\theta}{2}}{4E^2 \sin^4 \frac{\theta}{2}} \frac{E'}{E} \left(\frac{G_E^p{}^2 + \tau G_M^p{}^2}{1 + \tau} + 2\tau G_M^p{}^2 \tan^2 \frac{\theta}{2} \right)$$

$$= \sigma_M f_{rec}^{-1} \left(A + B \tan^2 \frac{\theta}{2} \right) \quad \tau = \frac{Q^2}{4M^2}$$



- Recoil proton polarization measurement (*pol beam only*)

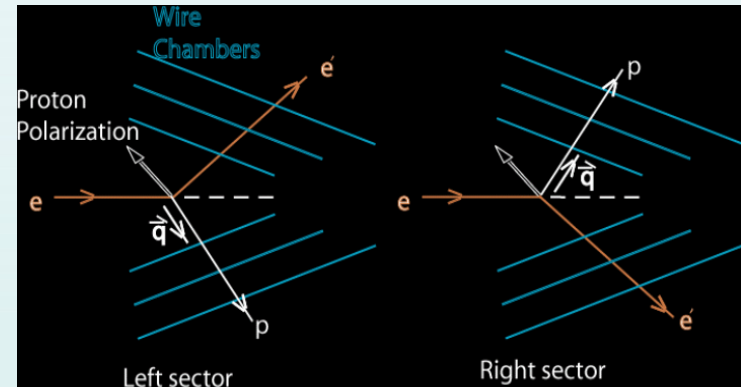
$$\frac{G_E^p}{G_M^p} = -\frac{P_t}{P_l} \frac{E + E'}{2M} \tan \frac{\theta}{2}$$

- Asymmetry (super-ratio) measurement

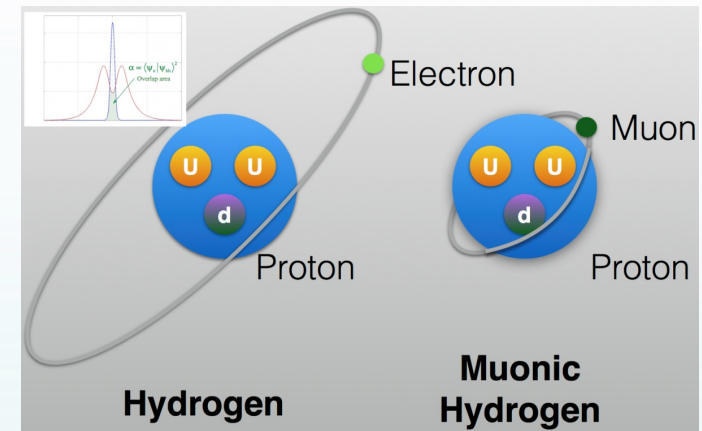
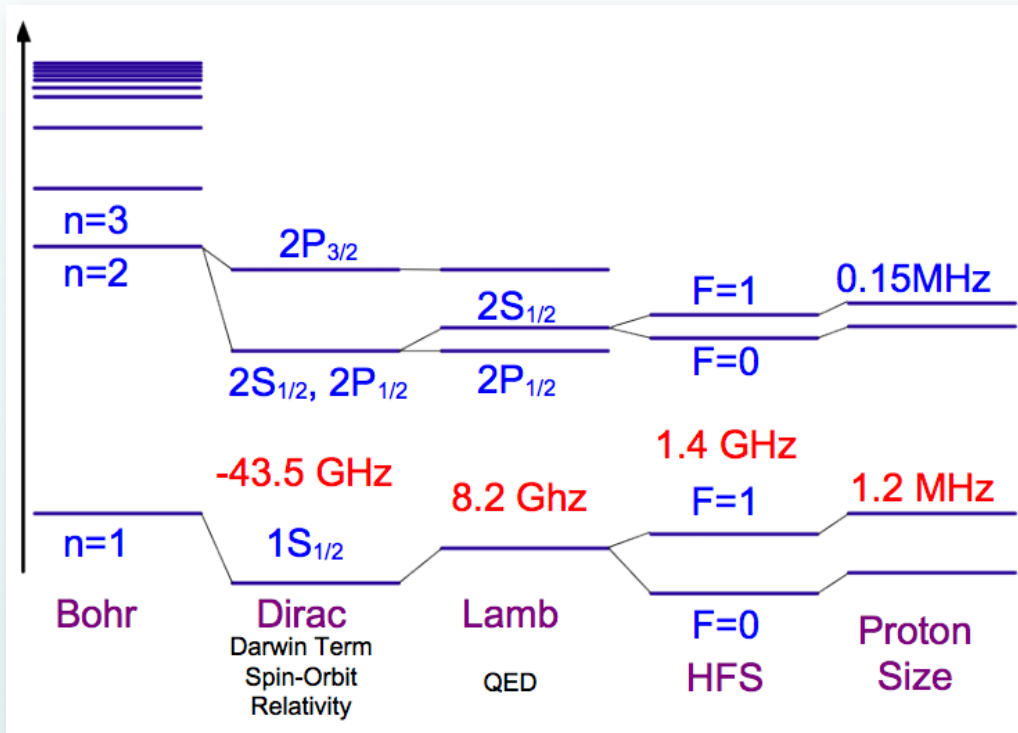
(*pol beam and pol target*)

$$R_A = \frac{A_1}{A_2} = \frac{a_1 - b_1 \cdot G_E^p/G_M^p}{a_2 - b_2 \cdot G_E^p/G_M^p}$$

$$A_{exp} = P_b P_t \frac{-2\tau v_{T'} \cos \theta^* G_M^p{}^2 + 2\sqrt{2\tau(1+\tau)} v_{TL'} \sin \theta^* \cos \phi^* G_M^p G_E^p}{(1+\tau) v_L G_E^p{}^2 + 2\tau v_T G_M^p{}^2}$$



Hydrogen Spectroscopy



$$\Delta E = -4\pi\alpha G_E^{\prime p}(0) |\psi_{n0}(0)|^2 \delta_{l0}$$

$$= 4\pi\alpha \frac{r_p^2}{6} |\psi_{n0}(0)|^2 \delta_{l0}.$$

The absolute frequency of H energy levels has been measured with an accuracy of 1.4 part in 10^{14} via comparison with an **atomic cesium fountain clock** as a primary frequency standard.

Yields Rydberg constant R_∞ (one of the most precisely known constants)

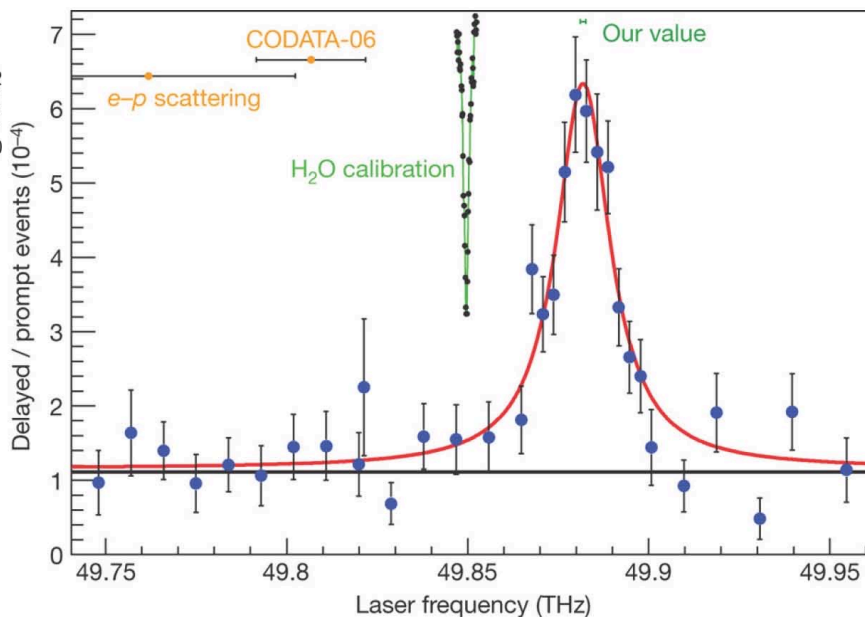
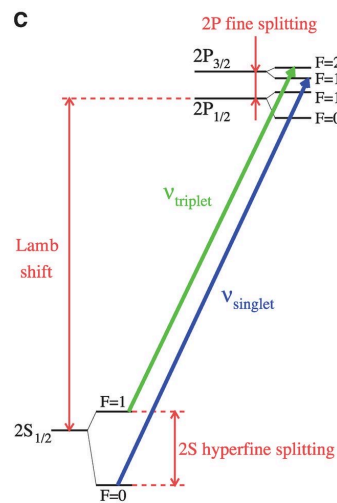
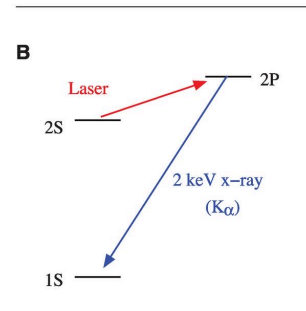
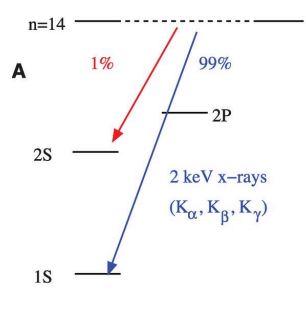
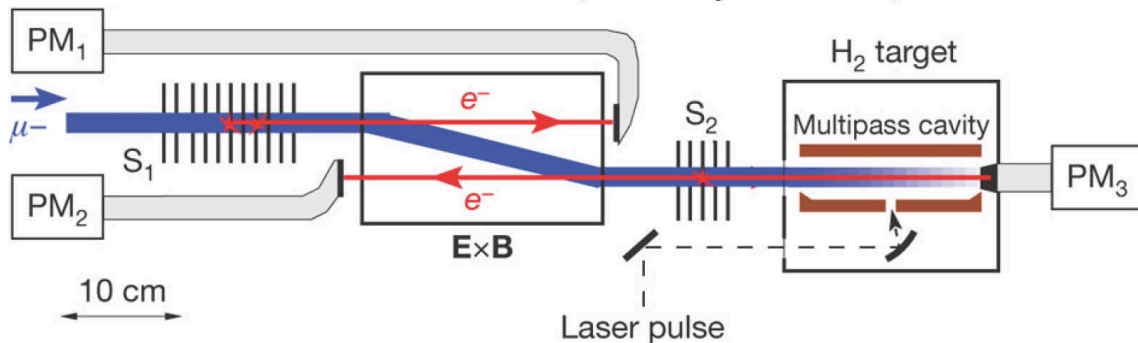
Comparing measurements to QED calculations that include corrections for the finite size of the proton can provide very precise value of the **rms proton charge radius**

Proton charge radius effect on the muonic hydrogen Lamb shift is 2%

Muonic hydrogen Lamb shift at PSI (2010, 2013)



Nature **466**, 213-216 (8 July 2010)

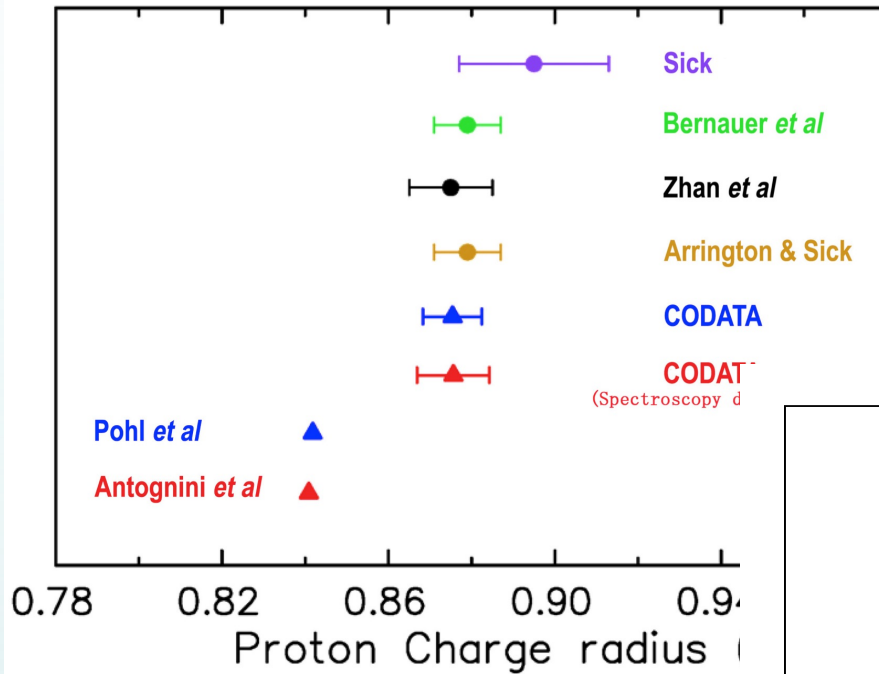


2010 value is $r_p = 0.84184(67)$ fm

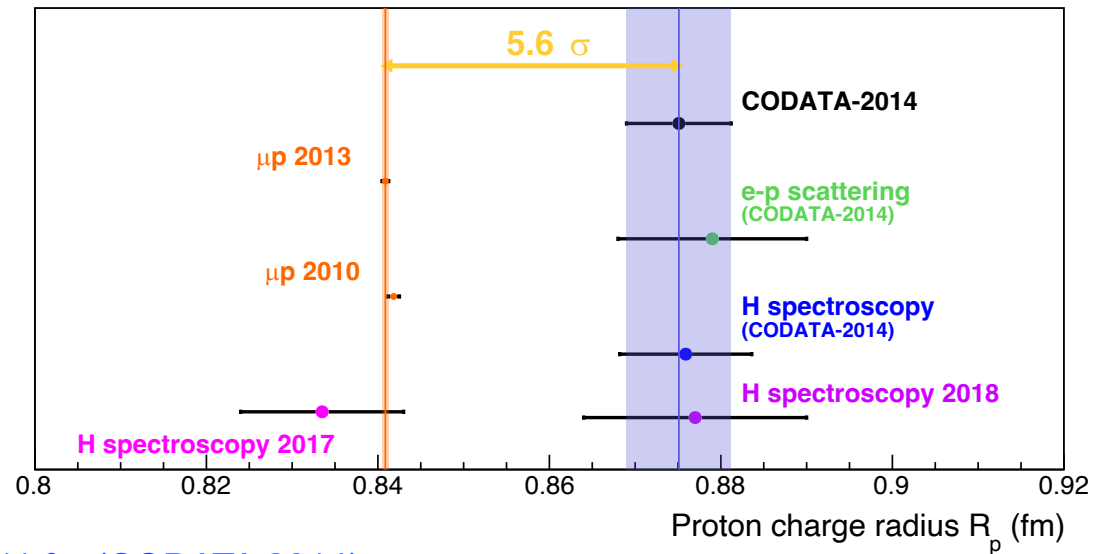
$r_p = 0.84087(39)$ fm, A. Antognini *et al.*, *Science* **339**, 417 (2013)

A. Antognini talk EFB25

The situation on the Proton Charge Radius in 2013 and 2018



This proton charge radius puzzle triggered intensive experimental and theoretical efforts worldwide in the last decade or so



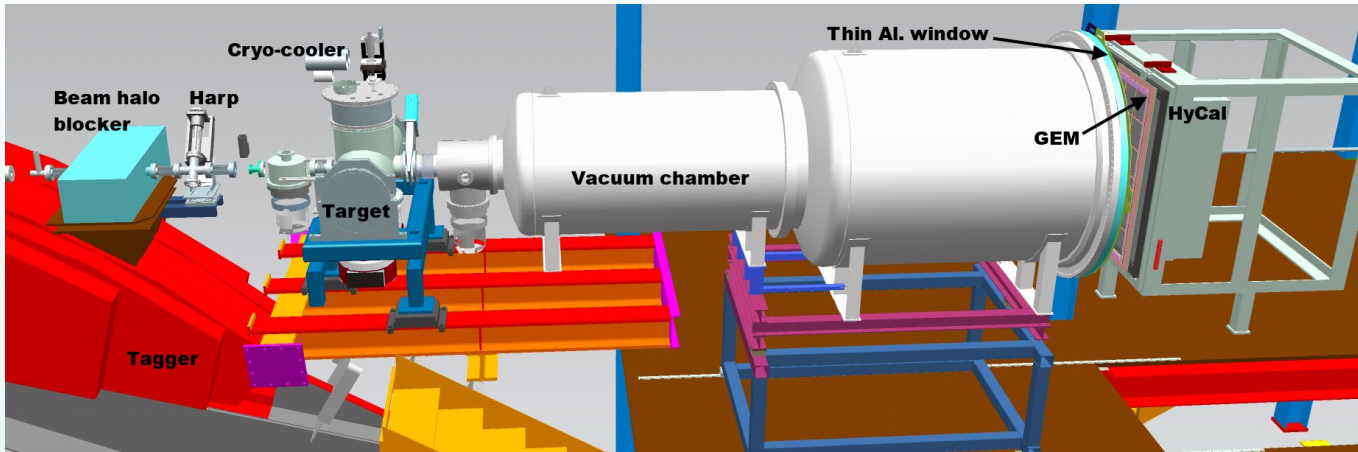
- Electron scattering: 0.879 ± 0.011 fm (CODATA 2014)
- Muon spectroscopy: 0.8409 ± 0.0004 fm (CREMA 2010, 2013)
- H spectroscopy (2017): 0.8335 ± 0.0095 fm (A. Beyer et al. Science 358(2017) 6359)
- H spectroscopy (2018): 0.877 ± 0.013 fm (H. Fleurbaey et al. PRL.120(2018) 183001)

ep scattering (ISR): $0.870 \pm 0.014_{\text{stat.}} \pm 0.024_{\text{syst.}} \pm 0.003_{\text{mod.}}$ (Mihovilovic 2019)
(not shown)

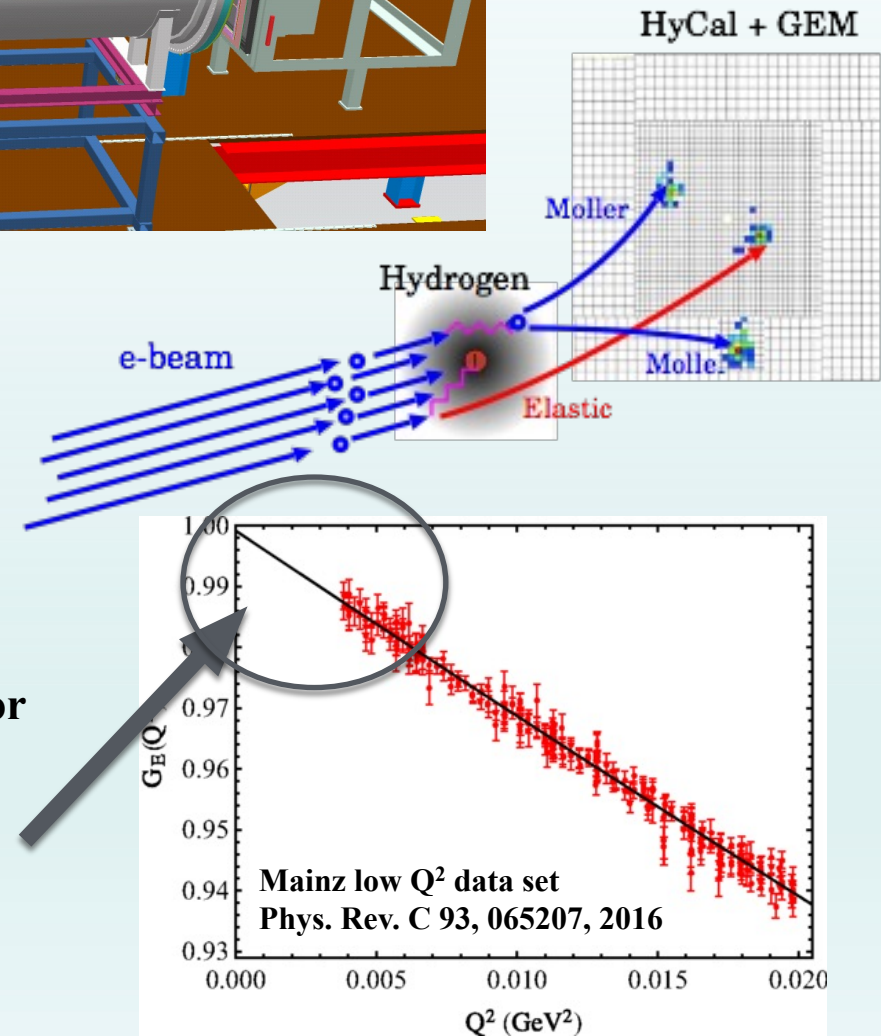
H. Gao EFB25

The PRad Experiment in Hall B at JLab

PRad
ton
Radius

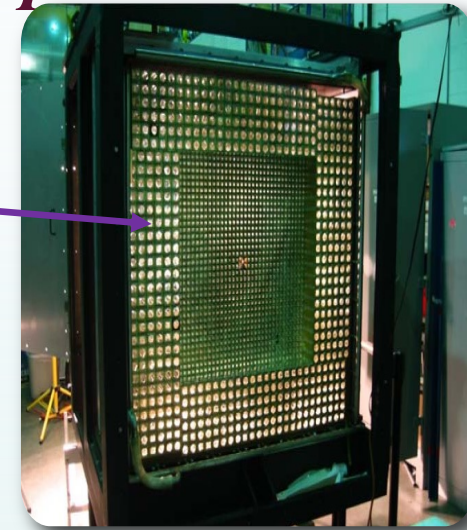
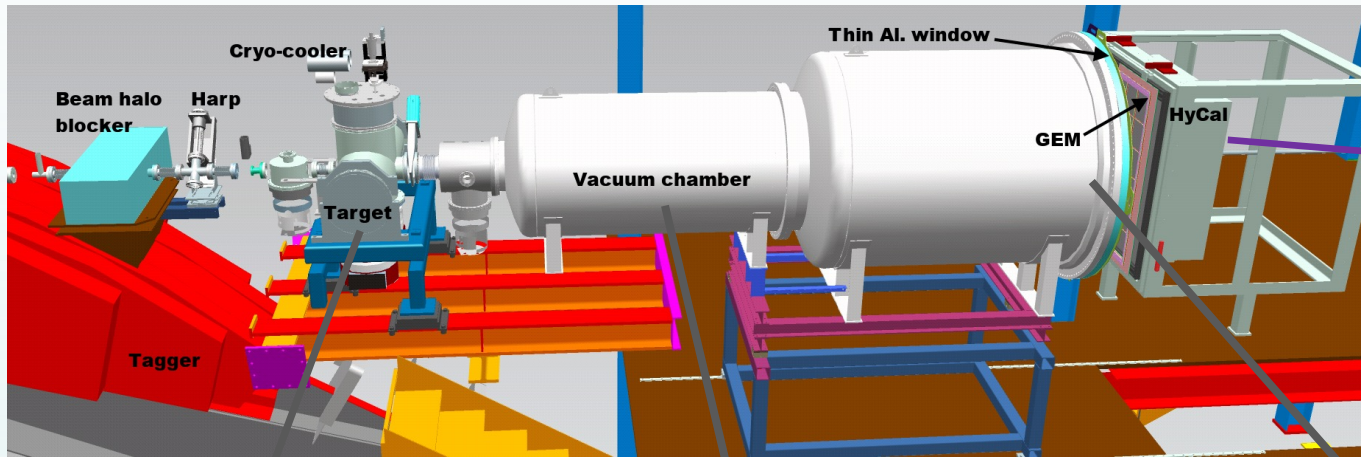


- High resolution, large acceptance, hybrid HyCal calorimeter (**PbWO₄** and **Pb-Glass**)
- Windowless H₂ gas flow target
- Simultaneous detection of elastic and Moller electrons
- Q² range of **2x10⁻⁴ – 0.06 GeV²**
- XY – veto counters replaced by GEM detector
- Vacuum chamber

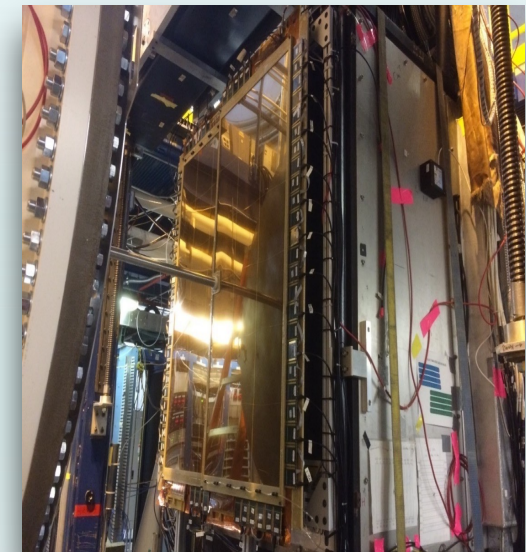
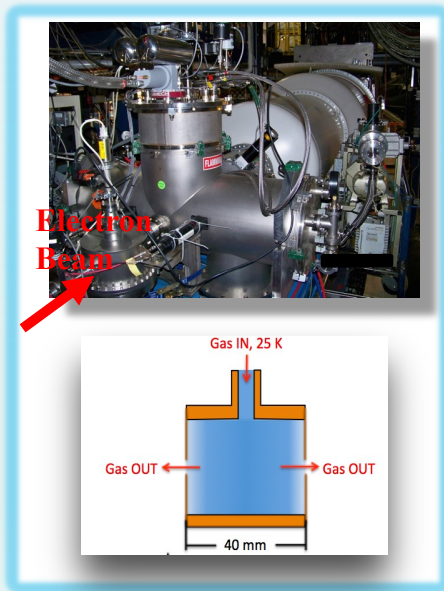


Spokespersons: **A. Gasparian (contact),
H. Gao, D. Dutta, M. Khandaker**

The *PRad* Experimental setup



I Larin, Y Y. Zhang, *et al.*,
Science 6490, 506

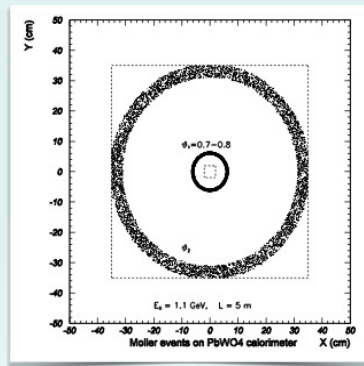


J. Pierce *et al.*, NIMA 1003, 165300 (2021)

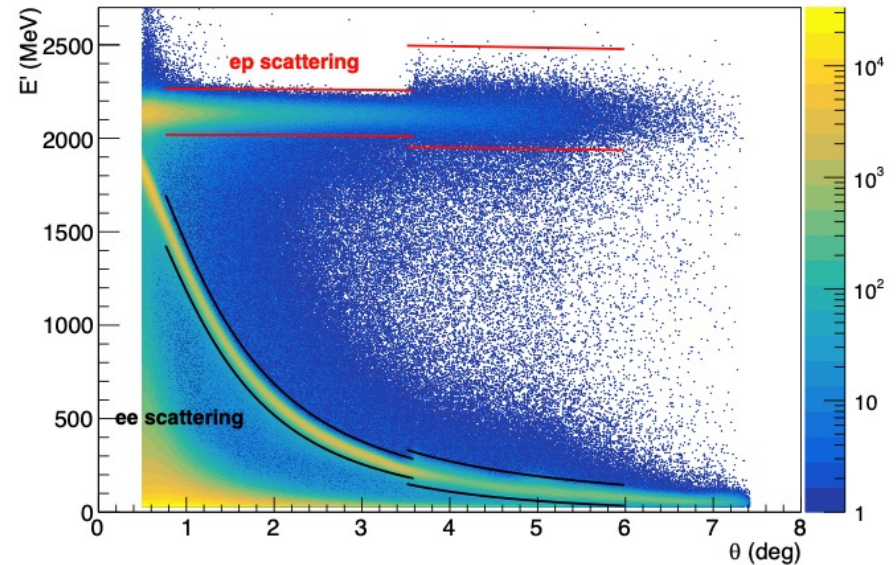
Analysis – Event Selection

Event selection method

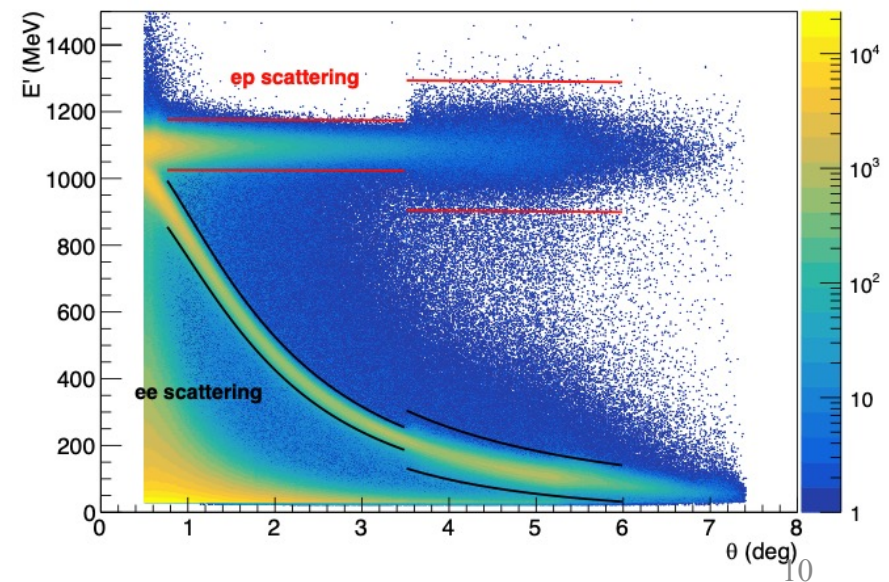
1. For all events, require hit matching between GEMs and HyCal
2. For ep and ee events, apply angle-dependent energy cut based on kinematics
 1. Cut size depend on local detector resolution
3. For ee , if requiring double-arm events, apply additional cuts
 1. Elasticity
 2. Co-planarity
 3. Vertex z



Cluster energy E' vs. scattering angle θ (2.2GeV)

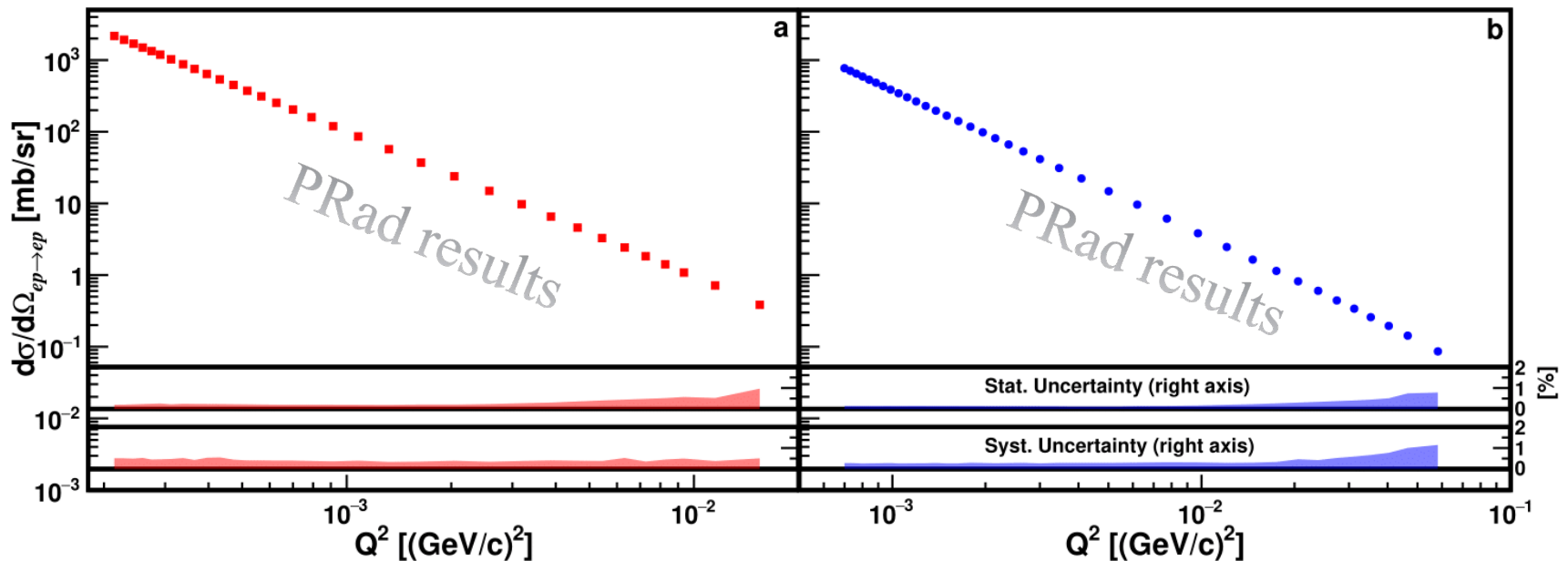


Cluster energy E' vs. scattering angle θ (1.1GeV)



Elastic ep Cross Sections

- Differential cross section v.s. Q^2 , with 2.2 and 1.1 GeV data
- Statistical uncertainties: $\sim 0.15\%$ for 2.2 GeV, $\sim 0.2\%$ for 1.1 GeV per point
- Systematic uncertainties: $0.3\% \sim 1.1\%$ for 2.2 GeV, $0.3\% \sim 0.5\%$ for 1.1 GeV (shown as shadow area)



Systematic uncertainties shown as bands

Proton Electric Form Factor G'_E (Normalized)

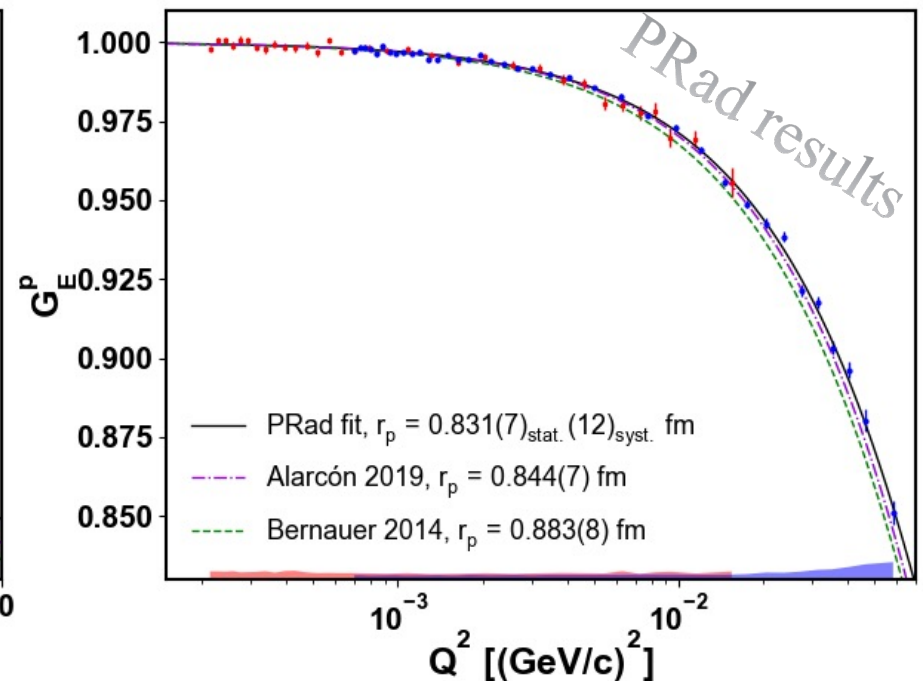
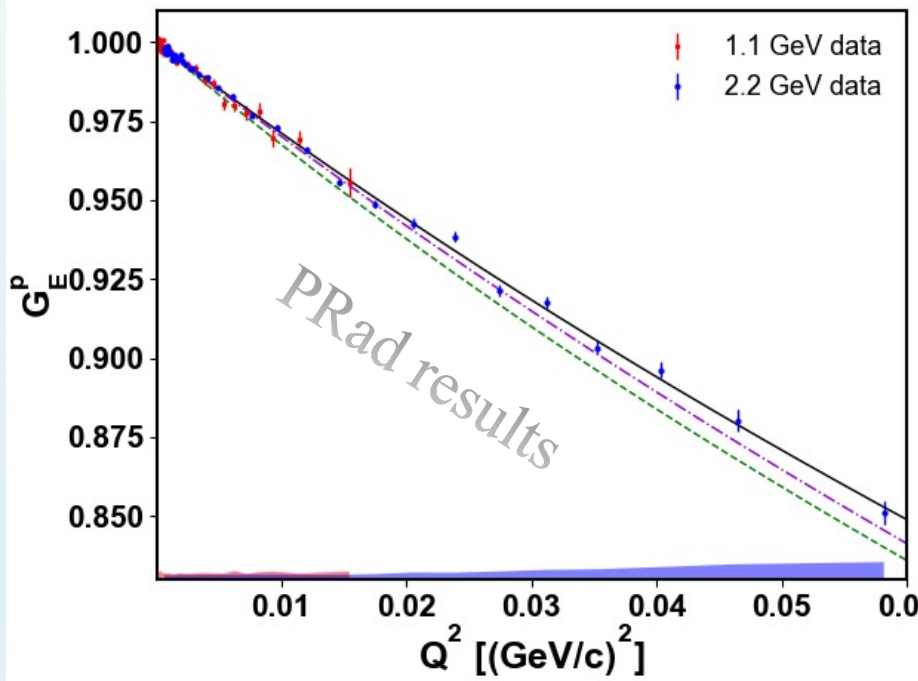
- n_1 and n_2 obtained by fitting PRad G_E to $\begin{cases} n_1 f(Q^2), & \text{for 1GeV data} \\ n_2 f(Q^2), & \text{for 2GeV data} \end{cases}$
- G'_E as normalized electric Form factor: $\begin{cases} G_E/n_1, & \text{for 1GeV data} \\ G_E/n_2, & \text{for 2GeV data} \end{cases}$
- PRad fit shown as $f(Q^2)$

Using rational (1,1)

$$f(Q^2) = \frac{1 + p_1 Q^2}{1 + p_2 Q^2}$$

Yan *et al.* PRC98,025204 (2018)

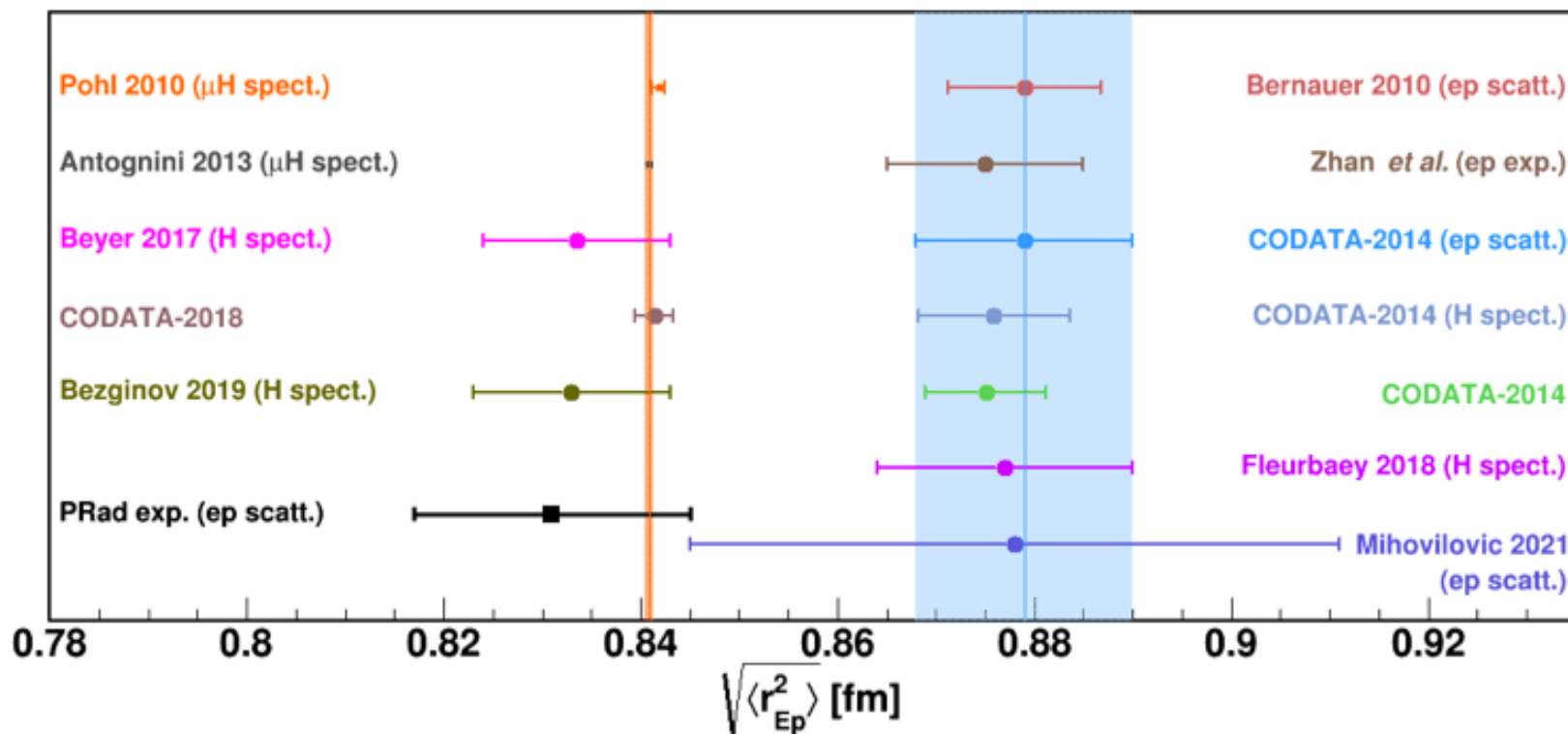
$$r_p = 0.831 \pm 0.007 \text{ (stat.)} \pm 0.012 \text{ (syst.) fm}$$



$$n_1 = 1.0002 \pm 0.0002 \text{ (stat.)} \pm 0.0020 \text{ (syst.)}, \quad n_2 = 0.9983 \pm 0.0002 \text{ (stat.)} \pm 0.0013 \text{ (syst.)}$$

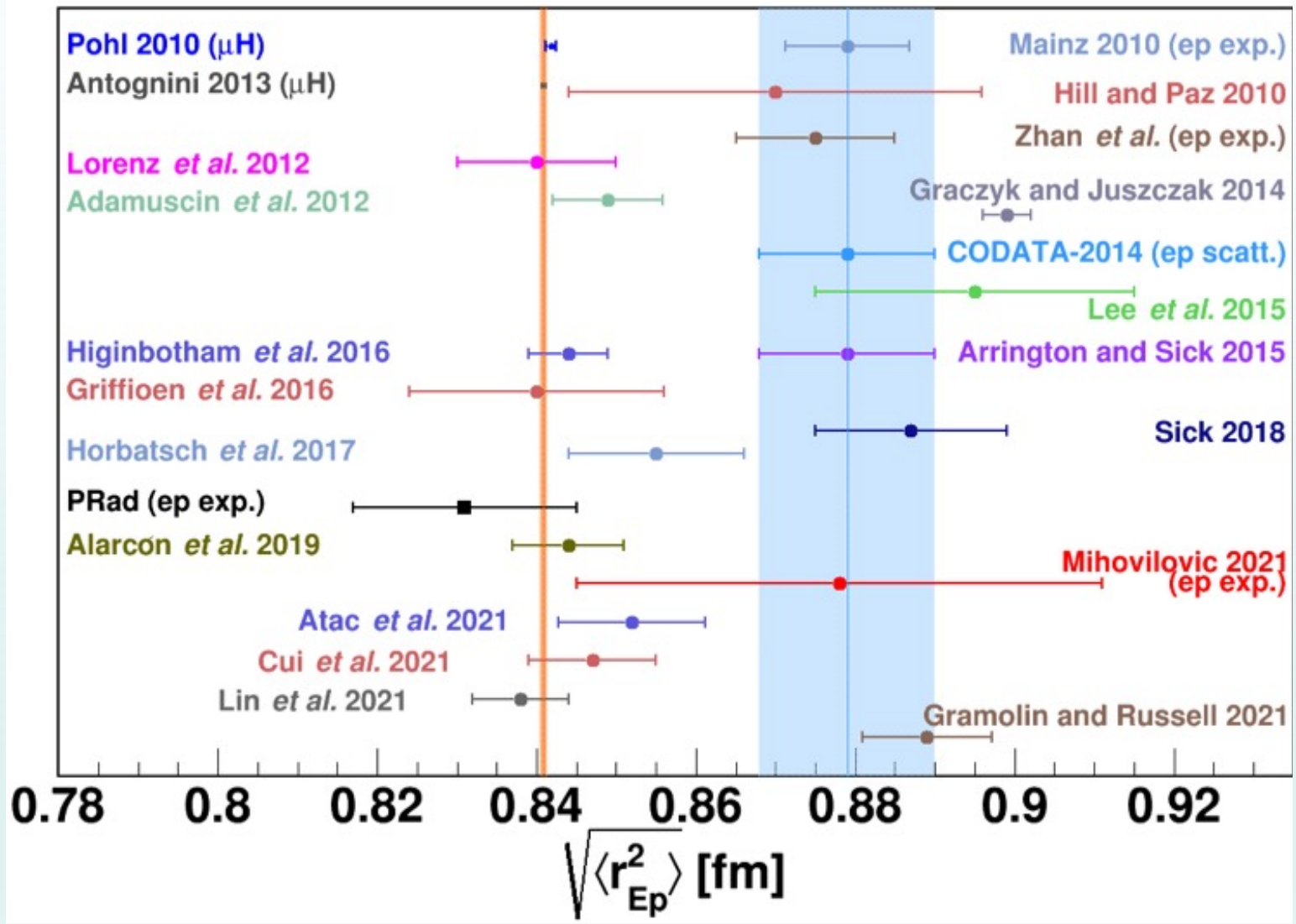
Proton radius at the time of PRad publication

- PRad result r_p : 0.831 ± 0.0127 fm, *Xiong et al., Nature 575, 147–150 (2019)*
- H Lamb Shift: 0.833 ± 0.010 fm *Bezginov et al., Science 365, 1007-1012 (2019)*
- CODATA 2018 value of r_p : 0.8414 ± 0.0019 fm, *E. Tiesinga et al., RMP 93, 025010(2021)*



CODATA has also shifted the value of the Rydberg constant.

(Re)analyses of e-p scattering data

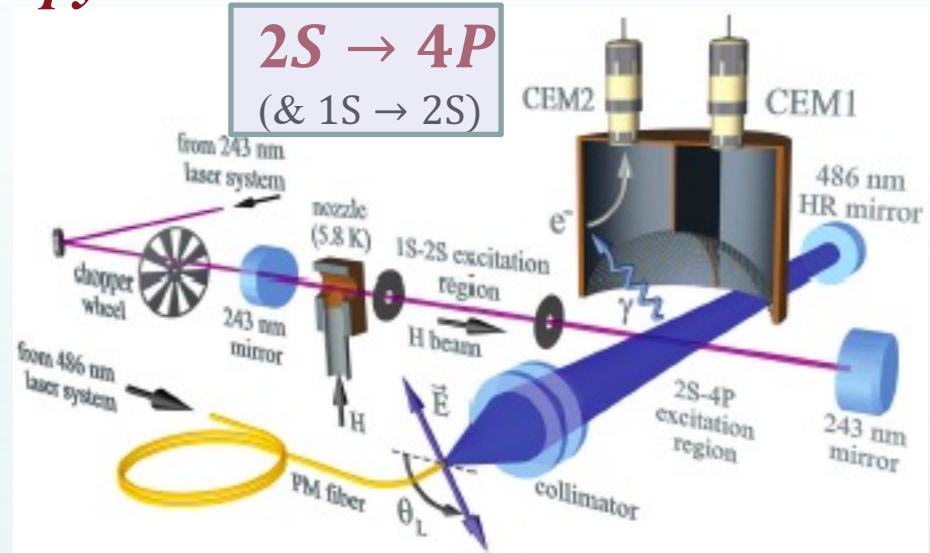
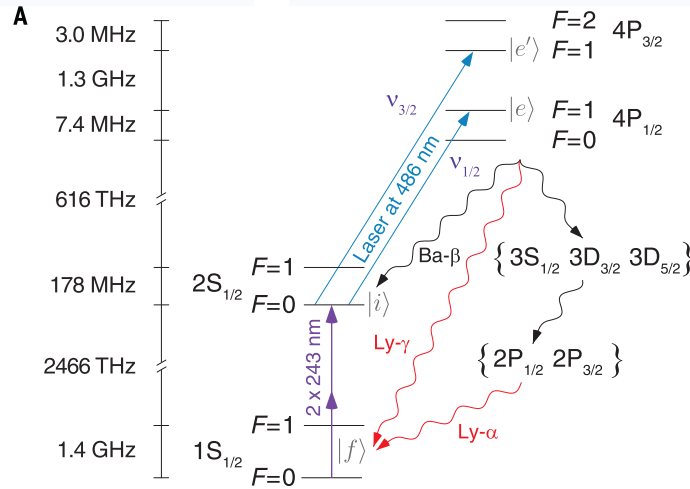


Gao and Vanderhaeghen, Rev. Mod. Phys. 94, 015002 (2022)

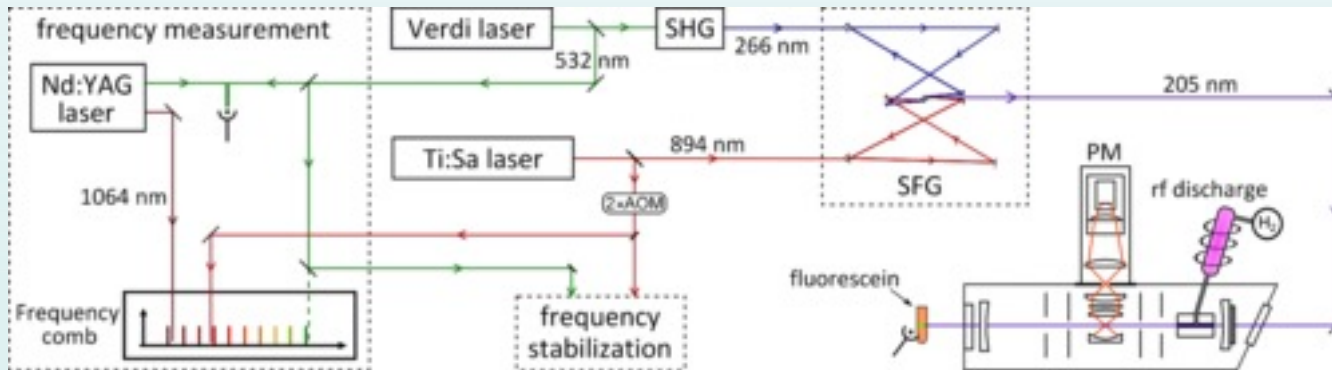
Cui *et al.*, arxiv:2204.05418, Chinese Physics C

Ulf-G. Meißner EFB25 talk

Ordinary hydrogen spectroscopy



$R_\infty = 10\,973\,731.568\,076(96) \text{ m}^{-1}, r_p = 0.8335(95) \text{ fm}$
Beyer *et al.*, Science 358, 79 (2017)

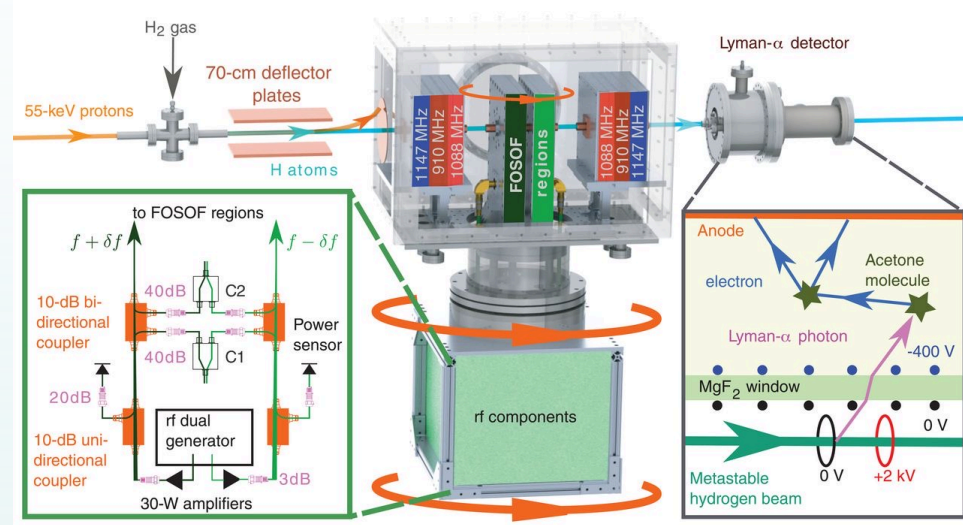
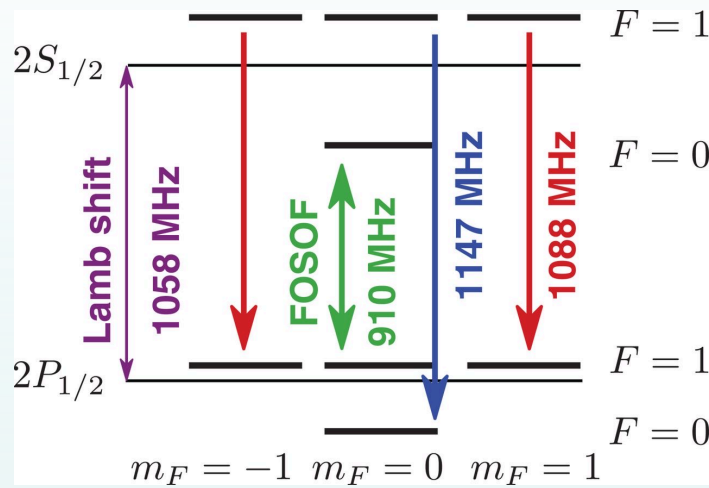


$R_\infty = 10\,973\,731.568\,53(14) \text{ m}^{-1}, r_p = 0.877(13) \text{ fm}$
Fleurbay *et al.* PRL 120, 183001 (2018)

$1S \rightarrow 3S$
($\& 1S \rightarrow 2S$)

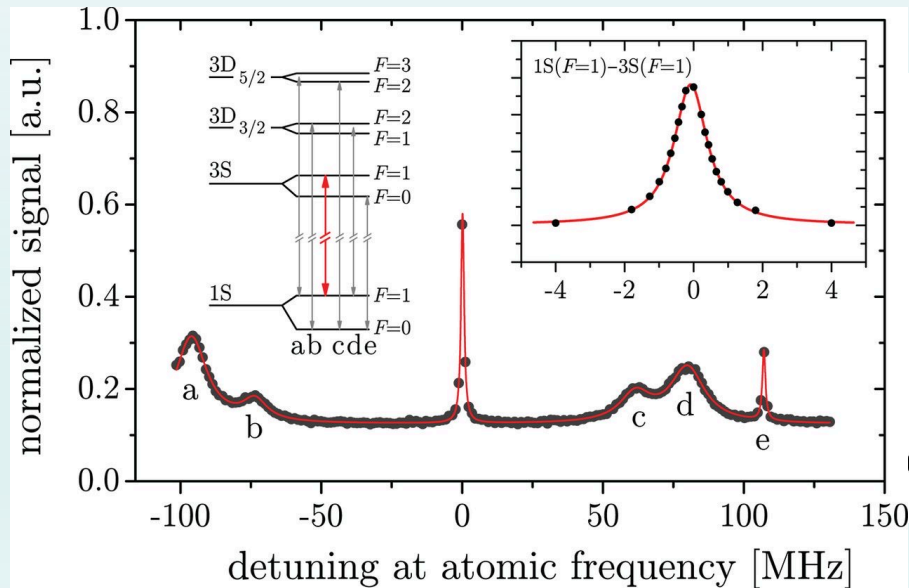
Parthey *et al.*, PRL 107, 203001 (2011)
Matveev *et al.* PRL 110, 230801 (2013)

More from ordinary hydrogen spectroscopy

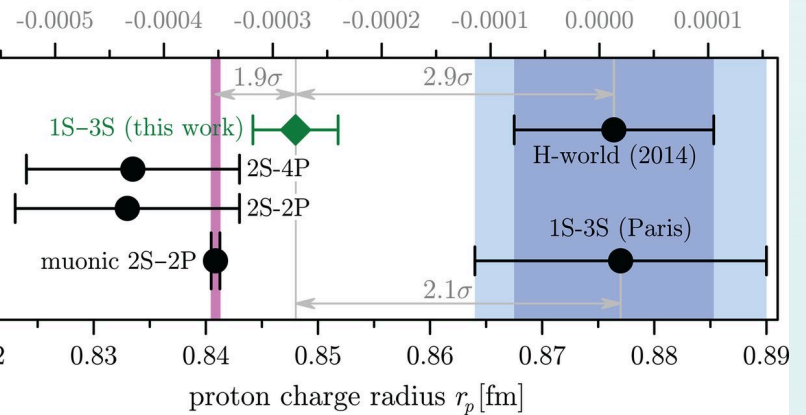


Bezginov *et al.*, Science 365, 1007 (2019)

$$r_p = 0.833(10) \text{ fm}$$



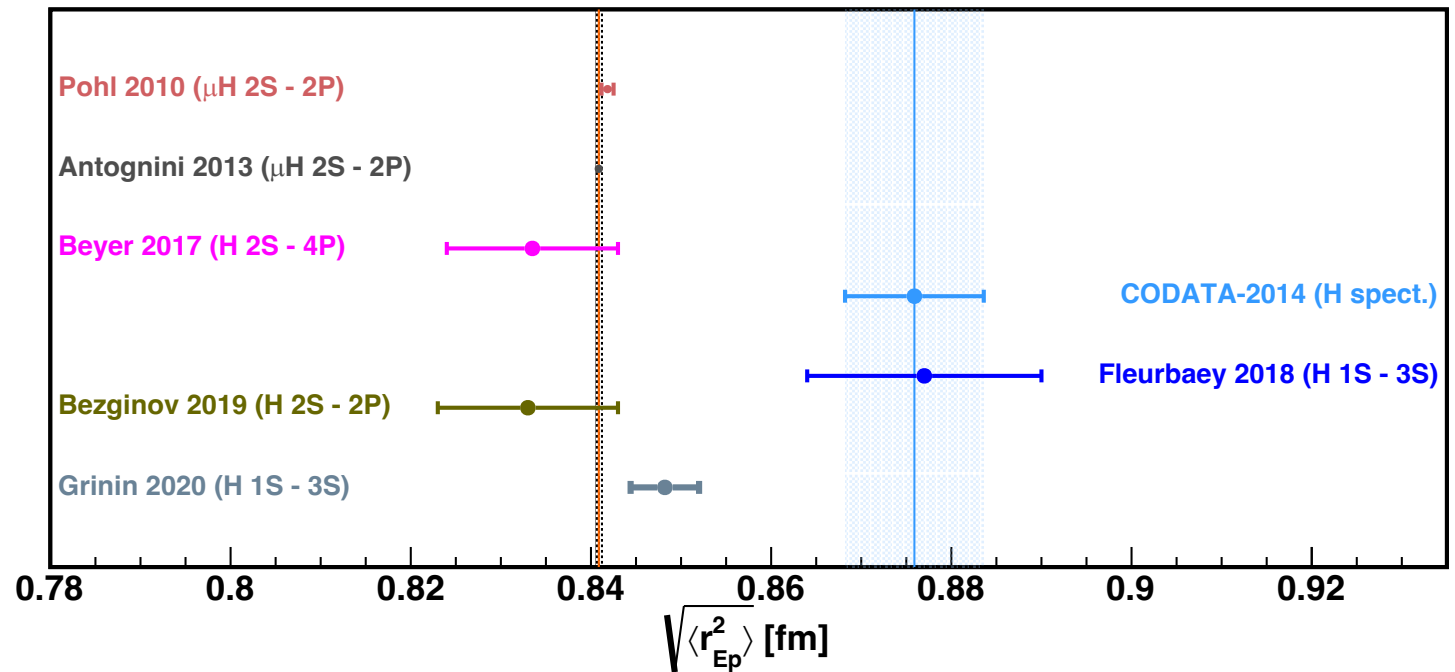
Rydberg constant $R_\infty - 10\,973\,731.568\,508 \text{ [m}^{-1}\text{]}$



Grinin *et al.*, Science 370, 1061 (2020)

$$r_p = 0.8482(38) \text{ fm}$$

Proton radius from ordinary and muonic H spectroscopy



Experiment	Type	Transition(s)	$\sqrt{\langle r_{Ep}^2 \rangle}$ (fm)	r_∞ (m^{-1})
Pohl 2010	μH	$2S_{1/2}^{F=1} - 2P_{3/2}^{F=2}$	0.84184(67)	
Antognini 2013	μH	$2S_{1/2}^{F=1} - 2P_{3/2}^{F=2}$ $2S_{1/2}^{F=0} - 2P_{3/2}^{F=1}$	0.84087(39)	
Beyer 2017	H	$2S - 4P$ with $(1S - 2S)$	0.8335(95)	10 973 731.568 076 (96)
Fleurbaey 2018	H	$1S - 3S$ with $(1S - 2S)$	0.877(13)	10 973 731.568 53(14)
Bezginov 2019	H	$2S_{1/2} - 2P_{1/2}$	0.833(10)	
Grinin 2020	H	$1S - 3S$ with $(1S - 2S)$	0.8482(38)	10 973 731.568 226(38)

Not included:

Brandt PRL128, 023001 (2022):
measured $2S_{1/2} - 8D_{5/2}$ transition
& used $1S - 2S$

Result:

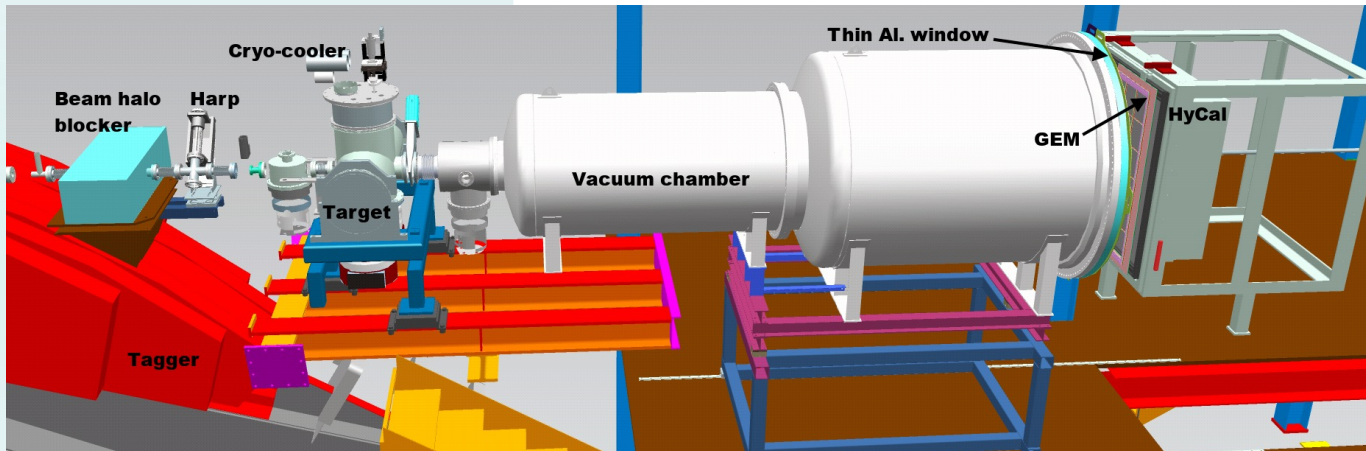
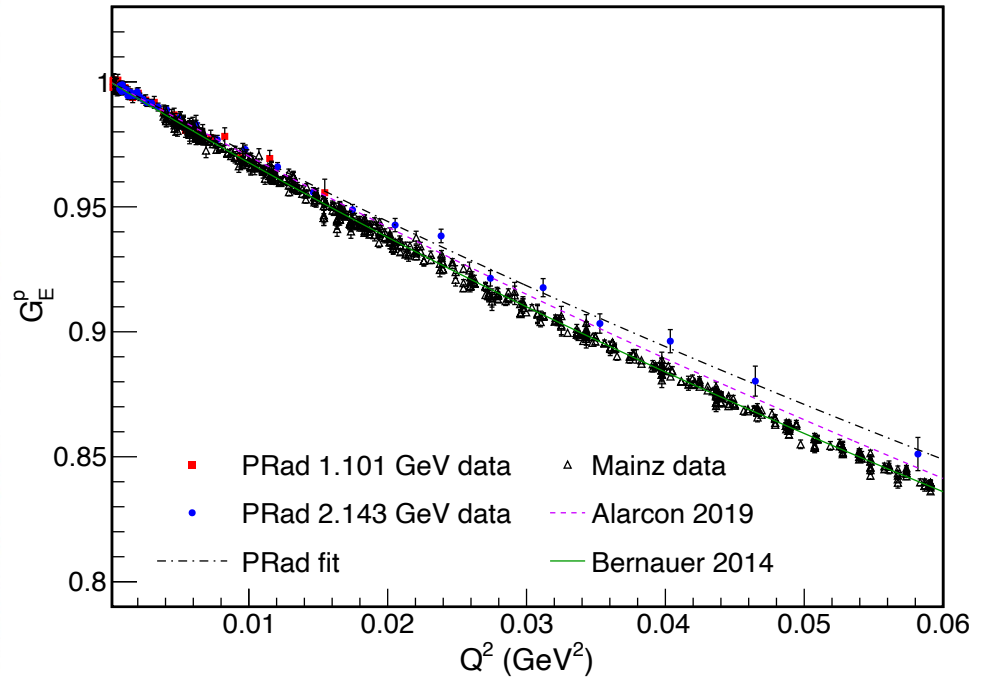
$r_p = 0.8584(51)$ fm
 $R_\infty = 10973731.568332(52)$ m^{-1} .

PRad-II: goals and approaches

- Reduce the uncertainty of the r_p measurement by a factor of **3.8!**
- Reach an unprecedented low values of Q^2 : $4 \times 10^{-5} \text{ (GeV/c)}^2$
- How?
 - Improving tracking capability by adding a second plane of tracking detector
 - Adding new rectangular cross shaped scintillator detectors to separate Moller from ep electrons in scattering angular range of 0.5^0 - 0.8^0
 - Upgrading HyCal and electronics for readout
 - Replacing lead glass blocks by PbWO_4 modules (uniformity, resolutions, inelastic channel)
 - Converting to FADC based readout
 - Suppressing beamline background
 - Improving vacuum
 - Adding second beam halo blocker upstream of the tagger
 - Reducing statistical uncertainties by a factor of 4 compared with PRad
 - Three beam energies: 0.7, 1.4 and 2.1 GeV – *0.7 GeV is critical to reach the lowest Q^2 ($4 \times 10^{-5} \text{ (GeV/c)}^2$)*
 - Improve radiative correction calculations by going to NNL order
 - Potential target improvement (*not used in projection*)

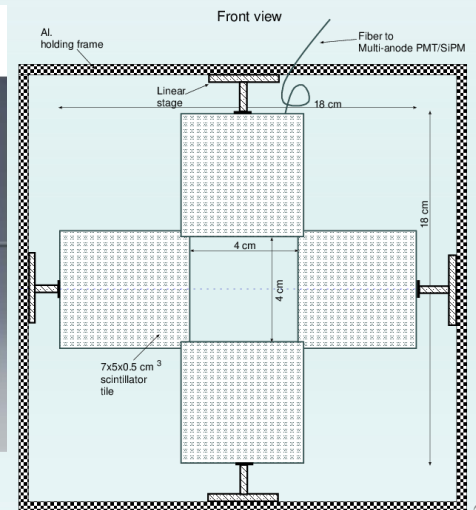
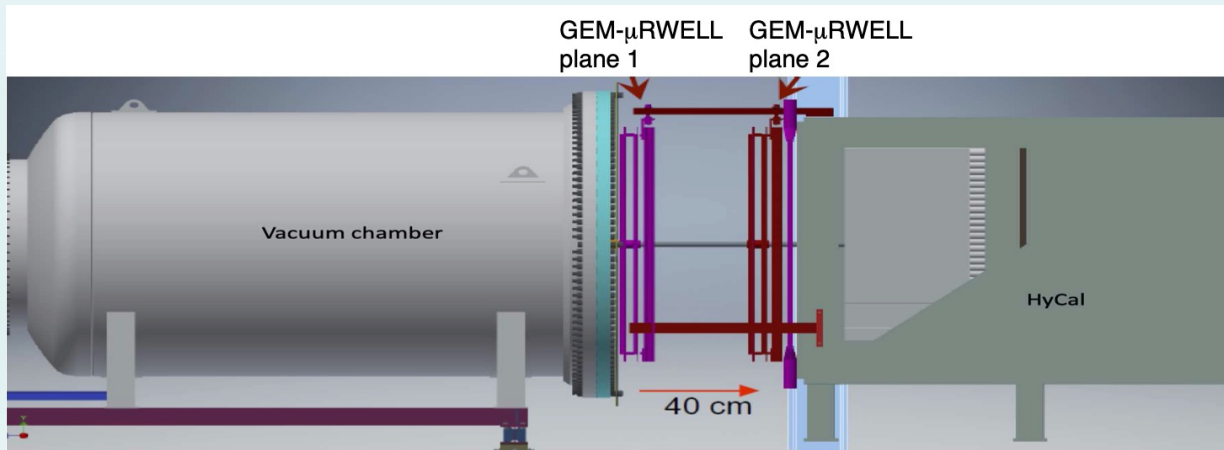
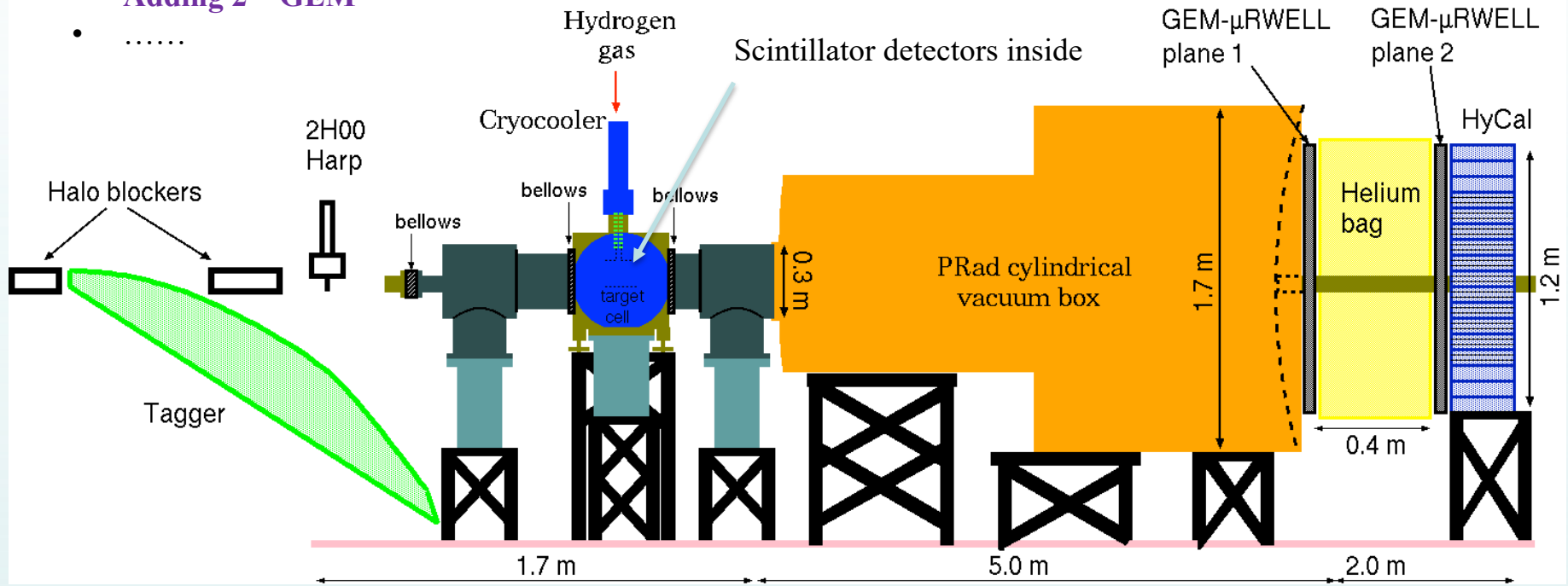
*Approved with the highest rating by the
JLab Program Advisory Committee in summer 2020*

e-p scattering: magnetic spectrometer and calorimetric method



PRad-II Experimental Setup (Side View)

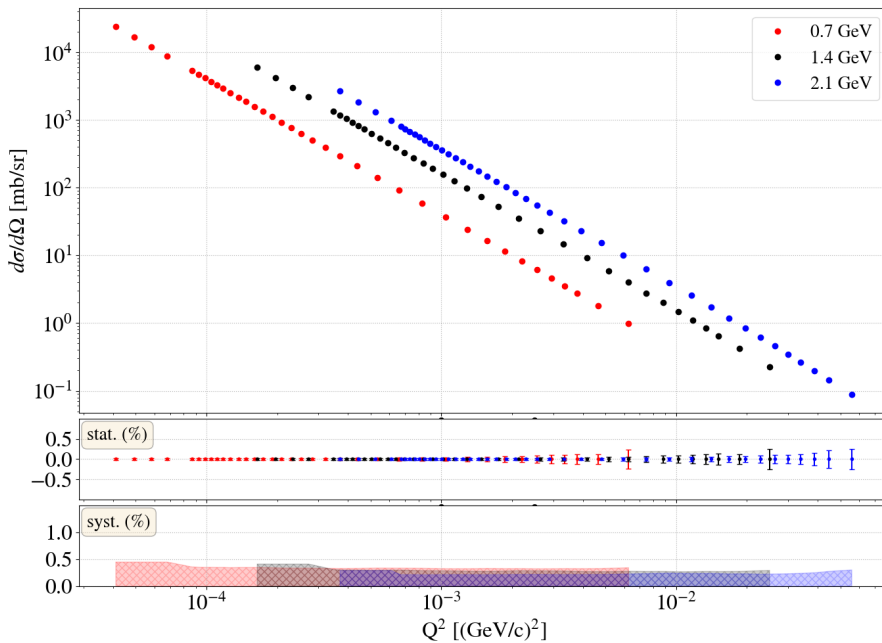
- Upgrade HyCal
- Adding 2nd GEM
-



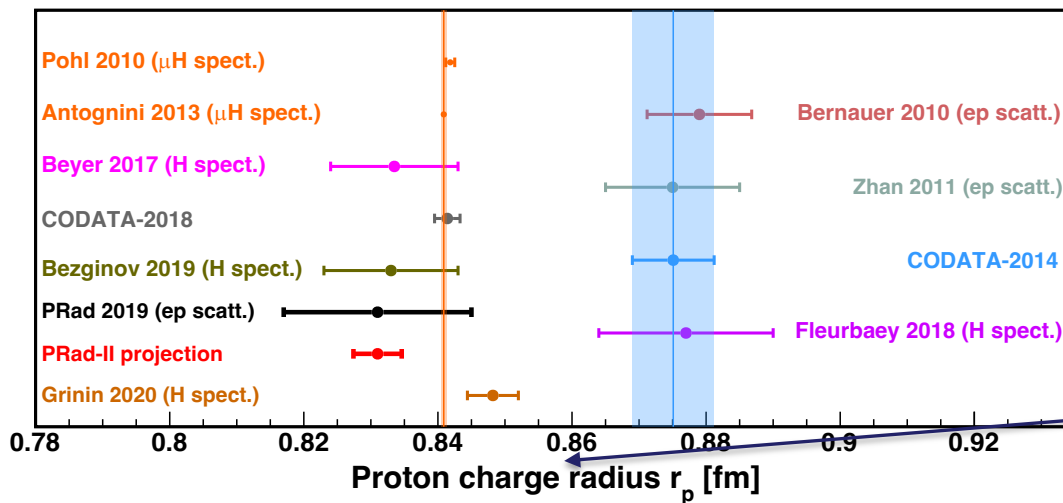
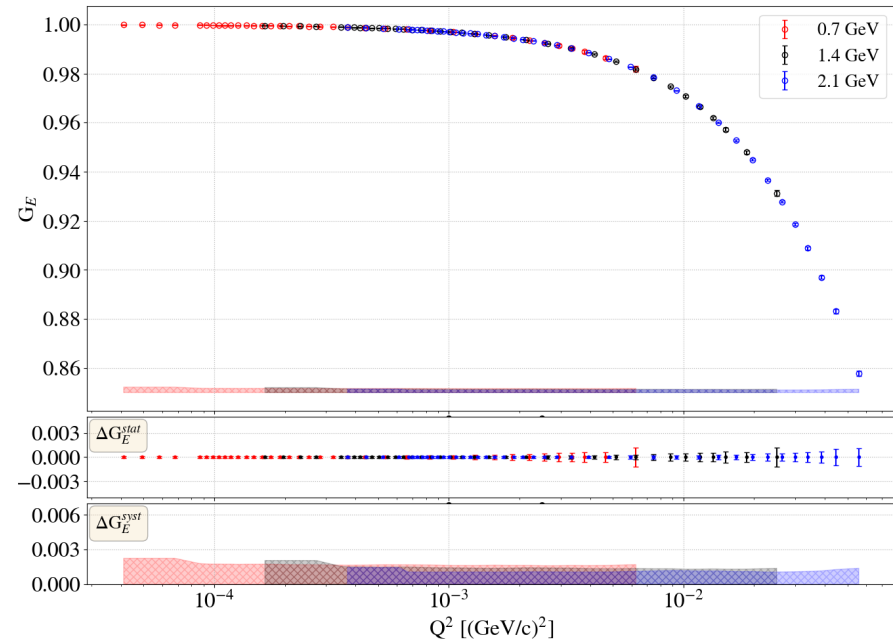
H. Gao EFB25

Projections for PRad-II

Differential Cross section



Electric form factor



- Nuclear deformation effects, Lin and Zou, arxiv:1910.13916
- New physics?

• **Most precise from ordinary hydrogen Lamb shift:**

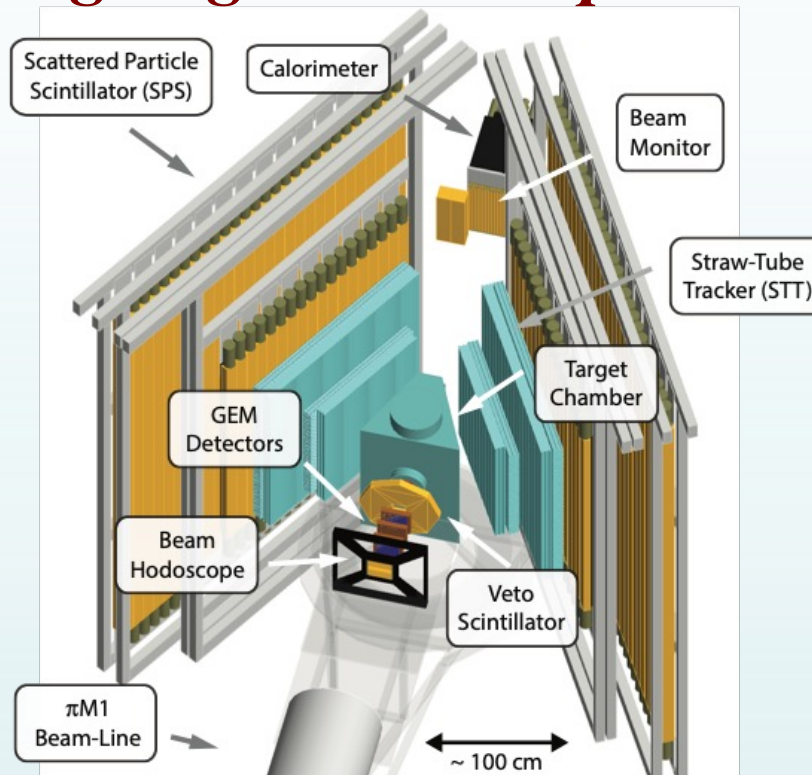
$$r_p = 0.8482 \pm 0.0038 \text{ fm}$$

Grinin *et al.*, Science **370**, 1061 (2020)

- **PRad-II: total uncertainty 0.0036 fm**

Gasparian *et al.* arXiv:2009.10510

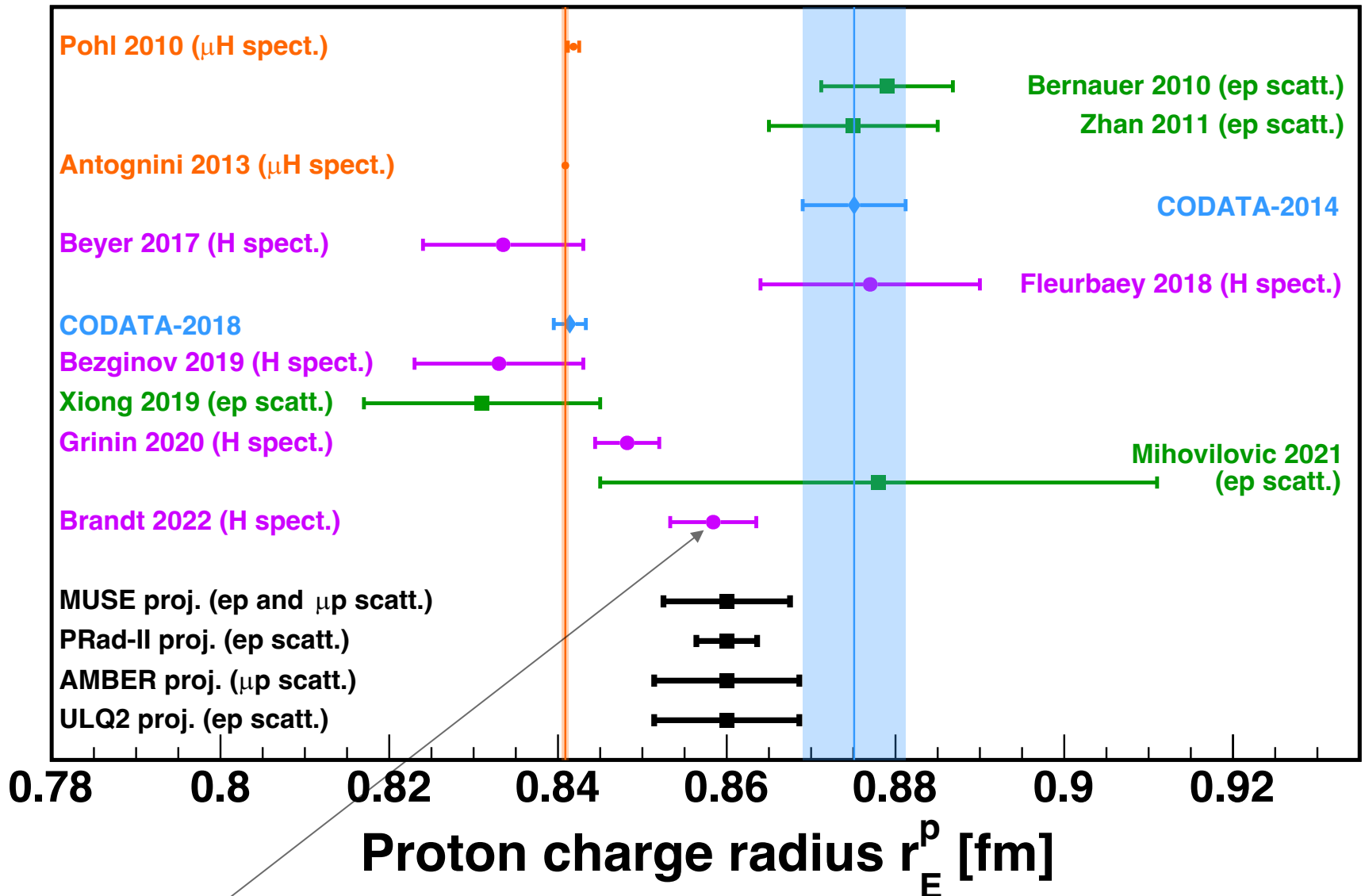
The ongoing MUSE Experiment at PSI



Beam momentum values:
115, 153, 210 MeV/c
Scattering angle: $20^\circ - 100^\circ$

Experiment	Beam	Laboratory	Q^2 (GeV/c) ²	δr_p (fm)	Status
MUSE	e^\pm, μ^\pm	PSI	0.0015 - 0.08	0.01	Ongoing
AMBER	μ^\pm	CERN	0.001 - 0.04	0.01	Future
PRad-II	e^-	Jefferson Lab	$4 \times 10^{-5} - 6 \times 10^{-2}$	0.0036	Future
PRES	e^-	Mainz	0.001 - 0.04	0.6% (rel.)	Future
A1@MAMI (jet target)	e^-	Mainz	0.004 - 0.085		Ongoing
MAGIX@MESA	e^-	Mainz	$\geq 10^{-4} - 0.085$		Future
ULQ ²	e^-	Tohoku University	$3 \times 10^{-4} - 8 \times 10^{-3}$	$\sim 1\%$ (rel.)	Future

The proton charge radius saga continues

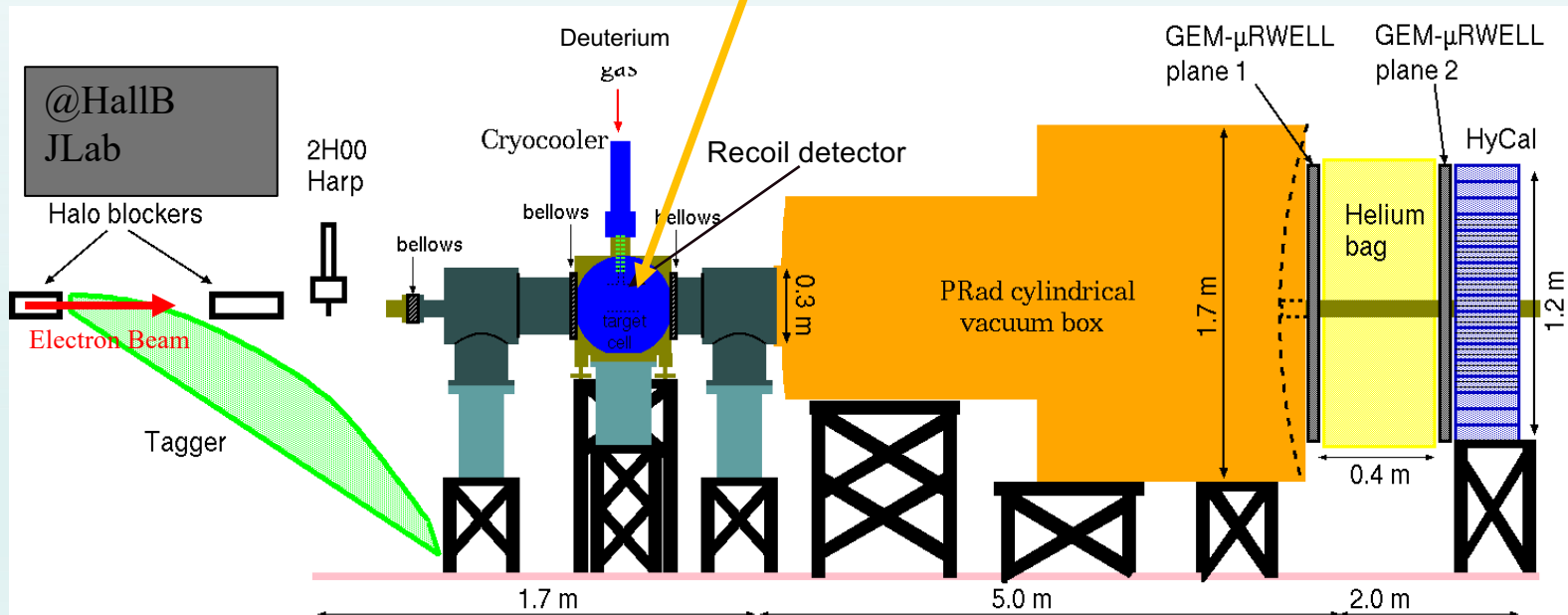


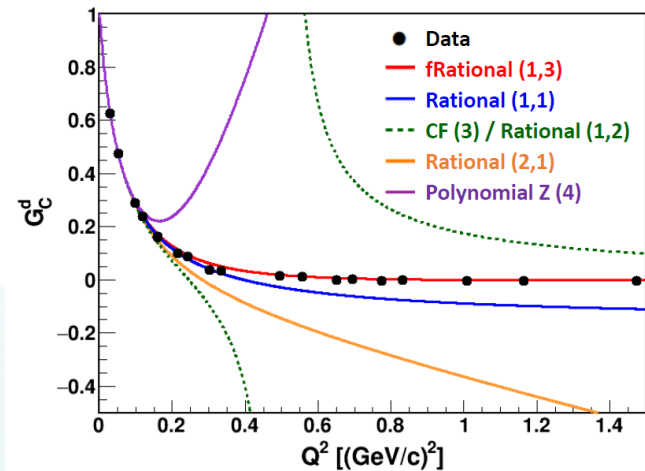
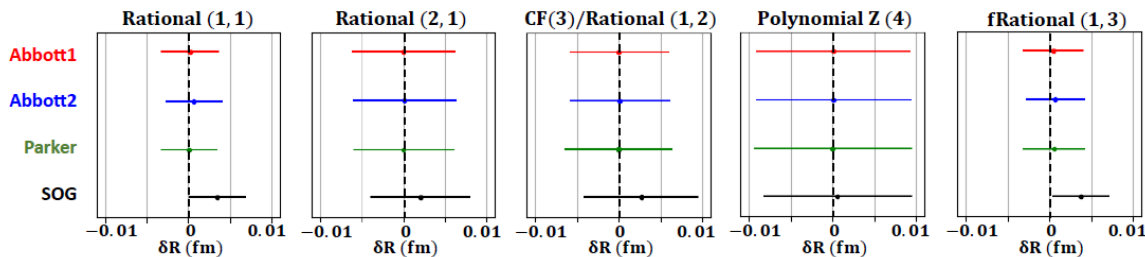
Brandt PRL128, 023001 (2022): measured $2S_{1/2} - 8D_{5/2}$ transition & used $1S - 2S$

The proposed DRad experiment at JLab

The DRad experiment

- Two beam energies, $E = 1.1$ and 2.2 GeV to measure $e-d$ elastic cross sections at very low Q^2 range: $[2 \times 10^{-4} - 5 \times 10^{-2}] (GeV/c)^2$.
- Experimental technique based on PRad-II, with a new two-layer cylindrical recoil detector for reaction elasticity





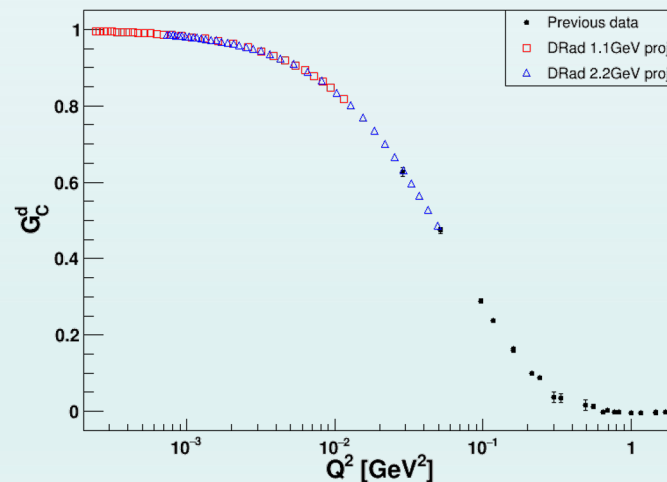
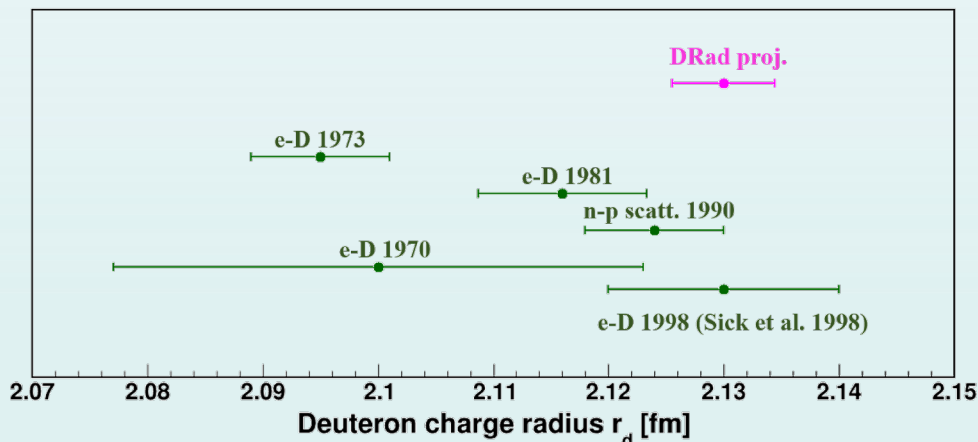
Proposed fitter: fixed Rational(1,3)

- Good ability to control the variance and acceptable bias
- Describe the G_C^d data at high Q^2 much better than the other fitters

$$f_{\text{fixed Rational}(1,3)}(Q^2) = p_0 \frac{1 + a_1 Q^2}{1 + b_1 Q^2 + b_{2,\text{fixed}} Q^4 + b_{3,\text{fixed}} Q^6}$$

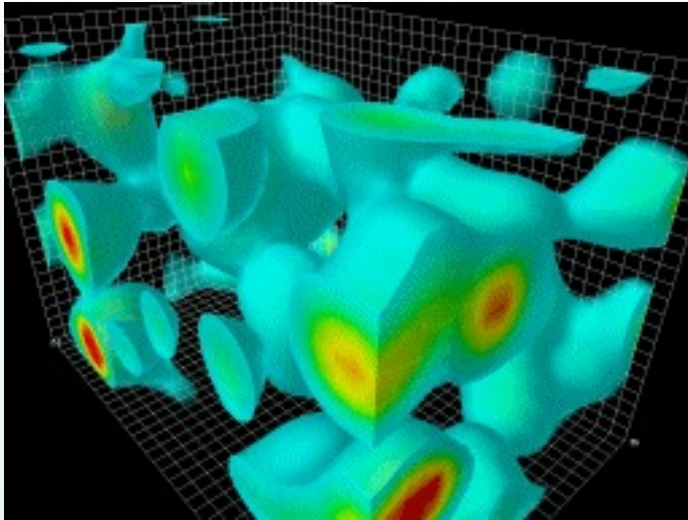
$$r_{\text{fit}} = \sqrt{6(a_1 - b_1)}$$

J. Zhou *et al.*, Phys. Rev. C 103, 024002

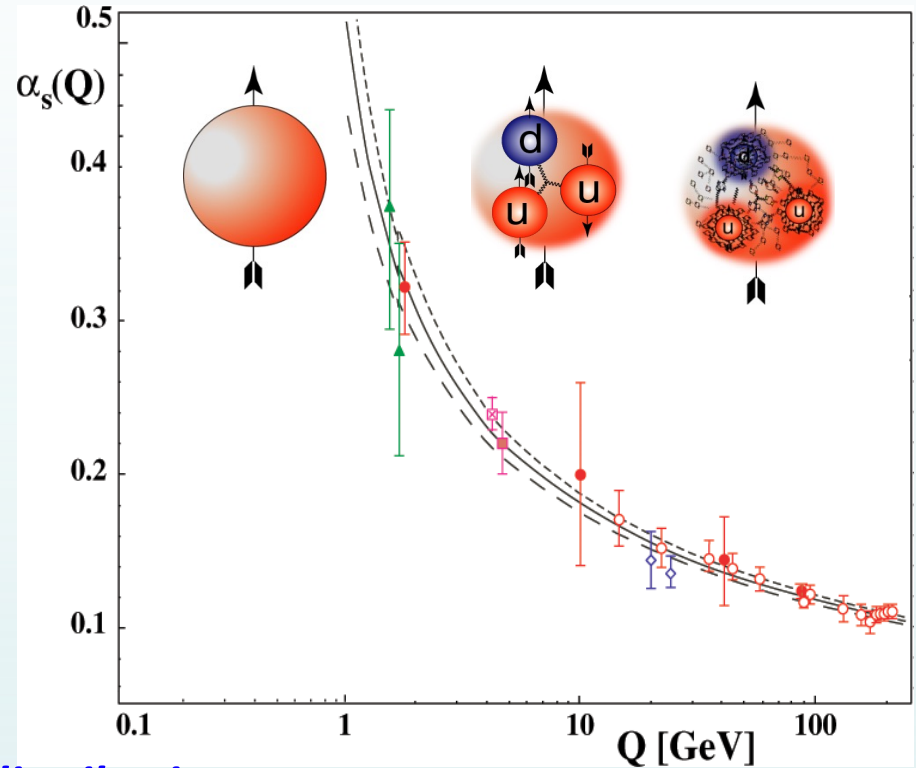


The most precise single measurement from e-d elastic scattering

QCD: still unsolved in non-perturbative region



Credit: D. Leinweber



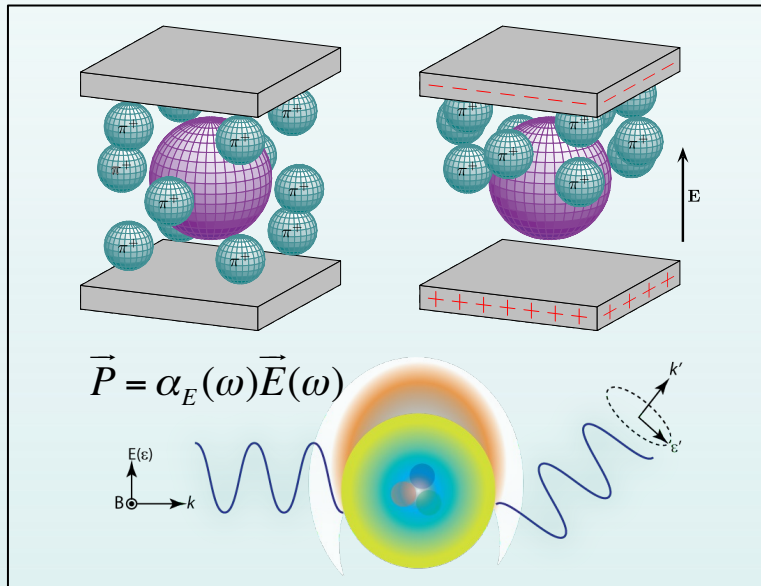
Gauge bosons: gluons

- Charge and magnetism (current) distribution
- Spin and mass decomposition
- Quark momentum and flavor distribution
- Polarizabilities
- Strangeness, charm content
- Three-dimensional structure
- more

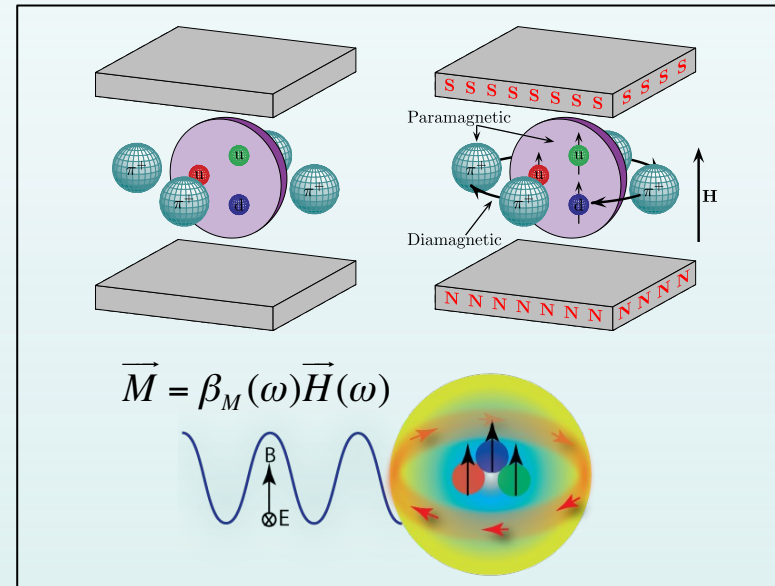
- 2004 Nobel prize for ``asymptotic freedom''
- **non-perturbative regime QCD ?????**
- One of the top 10 challenges for physics!
- QCD: Important for discovering new physics beyond SM
- Nucleon structure is one of the most active areas

Nucleon electromagnetic polarizabilities and nuclear Compton scattering

Electric polarizability (α_E)



Magnetic polarizability (β_M)



Polarizabilities characterize responses of the nucleon to the external EM field, another aspect related to its internal structure

In **nuclear Compton scattering**, the incident real photon acts as an external EM field applied to the nucleon

Differential cross section of Compton scattering $N(\gamma, \gamma')N'$

$$\frac{d\sigma}{d\Omega} = \underbrace{\frac{1}{2} \left(\frac{e^2 Z^2}{M_N} \right)^2 \left(\frac{\omega'}{\omega} \right)^2 [1 + g(\omega^2, \kappa)]}_{\text{Born term (nucleons are assumed as point-like particles)}} - \left(\frac{e^2 Z^2}{4\pi M_N} \right) \left(\frac{\omega'}{\omega} \right)^2 (\omega\omega') \left[\underbrace{\frac{1}{2}(\alpha + \beta)(1 + \cos\theta)^2}_{\text{dominant in forward-angle cross section}} + \underbrace{\frac{1}{2}(\alpha - \beta)(1 - \cos\theta)^2}_{\text{dominant in backward-angle cross section}} \right] + f(\omega^3, \gamma_1, \gamma_2, \gamma_3, \gamma_4) + \mathcal{O}(\omega^4)$$

eZ : nucleon charge ω : incident photon energy
 M_N : nucleon mass ω' : scattered photon energy
 κ : anomalous magnetic moment

To extract α and β of the **proton**:

- Measure the forward and backward Compton scattering cross sections
- Hydrogen targets

Differential cross section of Compton scattering $N(\gamma, \gamma')N'$

$$\frac{d\sigma}{d\Omega} = \underbrace{\frac{1}{2} \left(\frac{e^2 Z^2}{M_N} \right)^2 \left(\frac{\omega'}{\omega} \right)^2 [1 + g(\omega^2, \kappa)]}_{\text{Born term (nucleons are assumed as point-like particles)}} - \left(\frac{e^2 Z^2}{4\pi M_N} \right) \left(\frac{\omega'}{\omega} \right)^2 (\omega\omega') \left[\underbrace{\frac{1}{2}(\alpha + \beta)(1 + \cos\theta)^2}_{\text{dominant in forward-angle cross section}} + \underbrace{\frac{1}{2}(\alpha - \beta)(1 - \cos\theta)^2}_{\text{dominant in backward-angle cross section}} \right] + f(\omega^3, \gamma_1, \gamma_2, \gamma_3, \gamma_4) + \mathcal{O}(\omega^4)$$

More difficult!

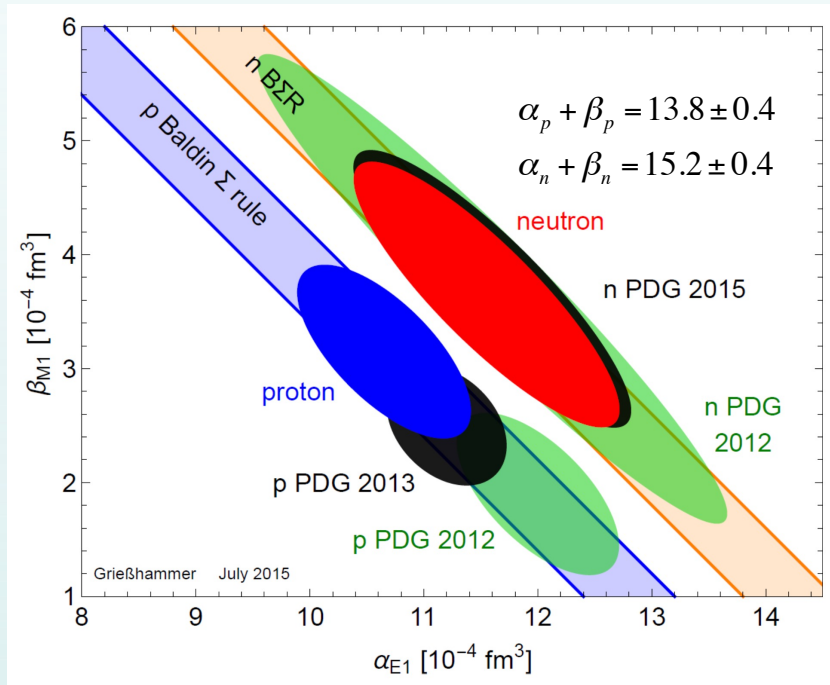
eZ : nucleon charge
 M_N : nucleon mass
 κ : anomalous magnetic moment
 ω : incident photon energy
 ω' : scattered photon energy

To extract α and β of the **neutron**:

- No stable free neutron target
- Neutron cross sections are small
- Effective neutron targets: ^2H , ^3He , ^4He , ...

Status of α_N and β_N from χEFT global extraction

Baldin sum rule (BSR):



$$\alpha_p = 10.65 \pm 0.35(stat) \pm 0.2(BSR) \pm 0.3(theory)$$

$$\beta_p = 3.15 \mp 0.35(stat) \pm 0.2(BSR) \pm 0.3(theory)$$

$$\alpha_n = 11.55 \pm 1.25(stat) \pm 0.2(BSR) \pm 0.8(theory)$$

$$\beta_n = 3.65 \mp 1.25(stat) \pm 0.2(BSR) \pm 0.8(theory)$$

L. S. Myers *et al.*, Phys. Rev. Lett. **113**, 262506 (2014)

H. W. Grießhammer, J. A. McGovern, D. R. Phillips, and G. Feldman, Prog. Part. Nucl. Phys. **67**, 841 (2012)

J. A. McGovern, D. R. Phillips, and H. W. Grießhammer, Eur. Phys. J. A **49**, 12 (2013)

H. W. Grießhammer, J. A. McGovern, and D. R. Phillips, Eur. Phys. J. A **52**, 139 (2016)

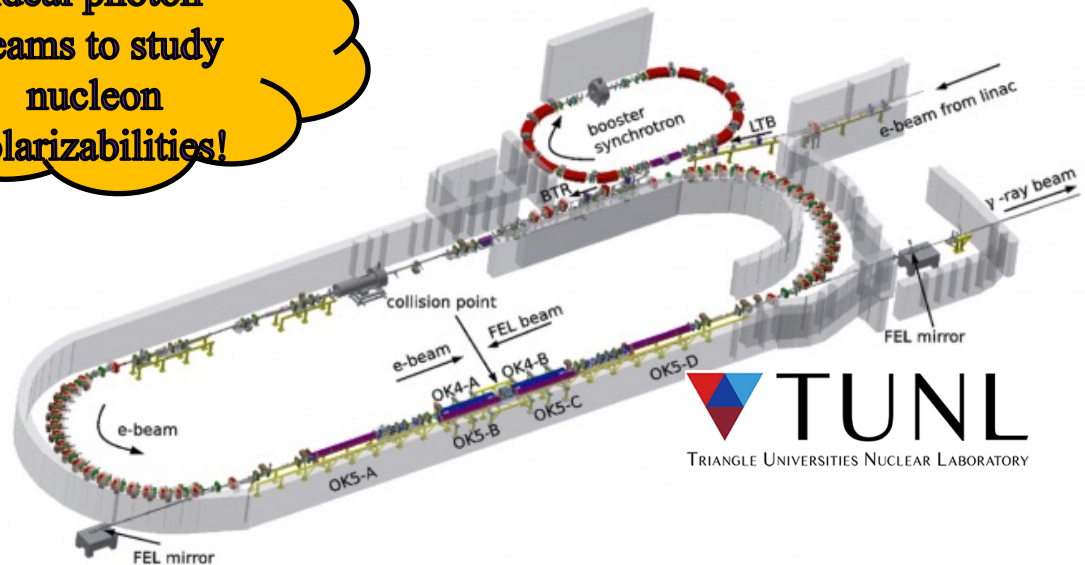
The High Intensity γ -Ray Source (HI γ S) facility at Duke University



- Photon beam energy: 1 - 120 MeV
- Nearly 100% circular/linear photon beam polarization
- Total flux: $\sim 10^{10}$ γ /s ($E_\gamma < 20$ MeV) and $\sim 10^8$ γ /s ($E_\gamma > 60$ MeV)

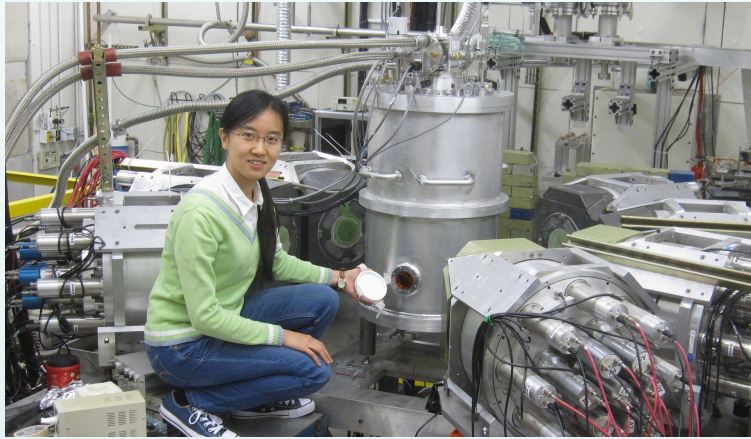
Ideal photon beams to study nucleon polarizabilities!

- Operated by Triangle Universities Nuclear Laboratory (TUNL)
- Free-electron laser (FEL)
- Compton backscattering
- Quasi-monoenergetic intense γ -ray beams



 **TUNL**
TRIANGLE UNIVERSITIES NUCLEAR LABORATORY

Experimental apparatus for Compton @ HI γ S

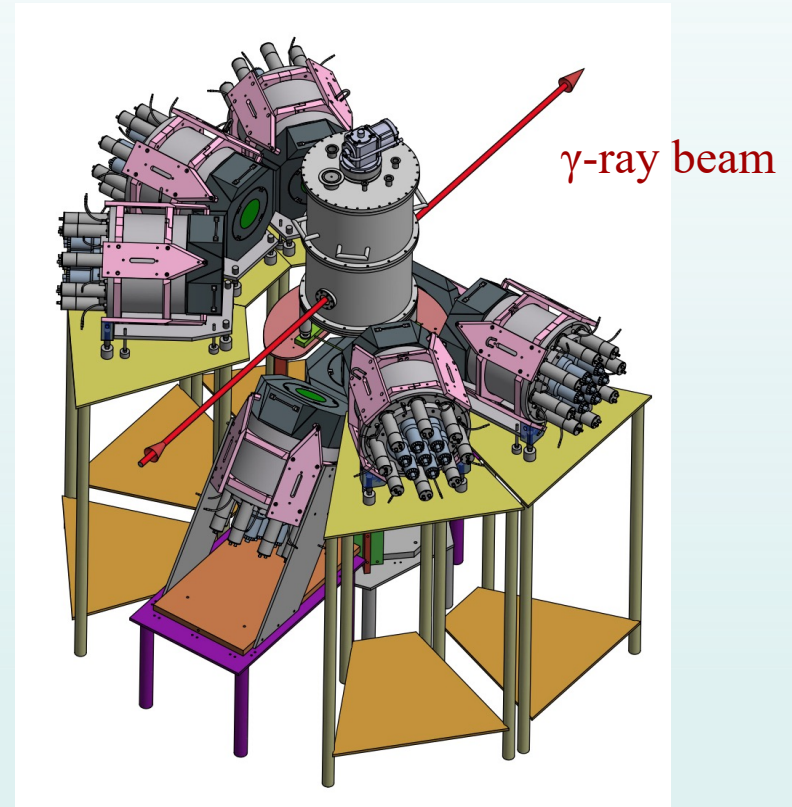


Detector array

- Eight NaI(Tl) core detectors
- $\theta = 55^\circ, 90^\circ, 125^\circ$
- $\phi = 0^\circ, 180^\circ, 270^\circ$
- Active shield structure

Cryogenic targets

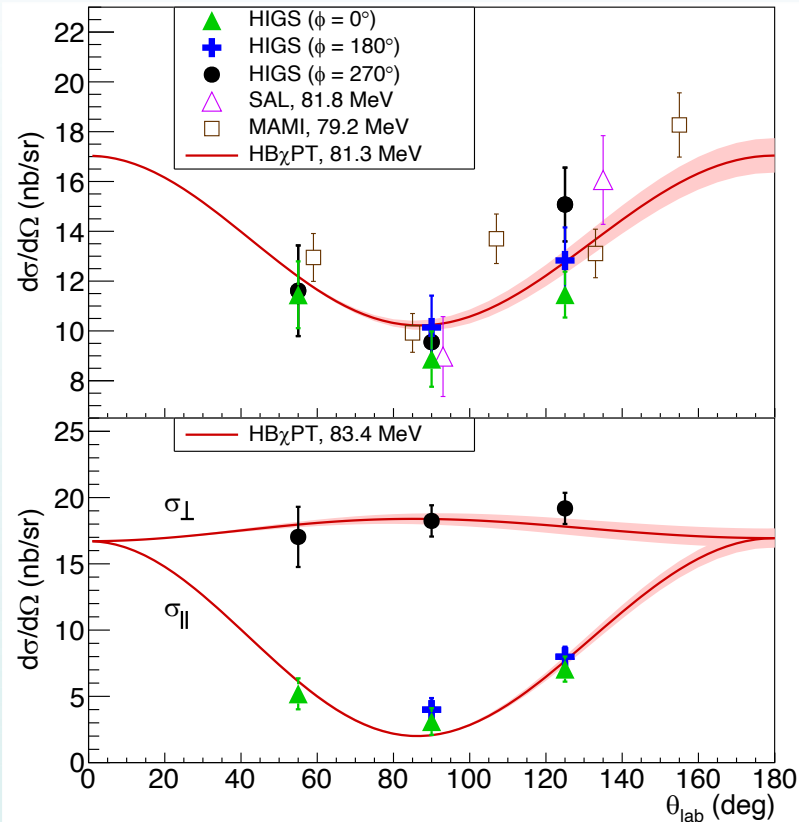
- liquid ^4He (LHe)
- Liquid hydrogen (LH $_2$)
- Liquid deuterium (LD $_2$)



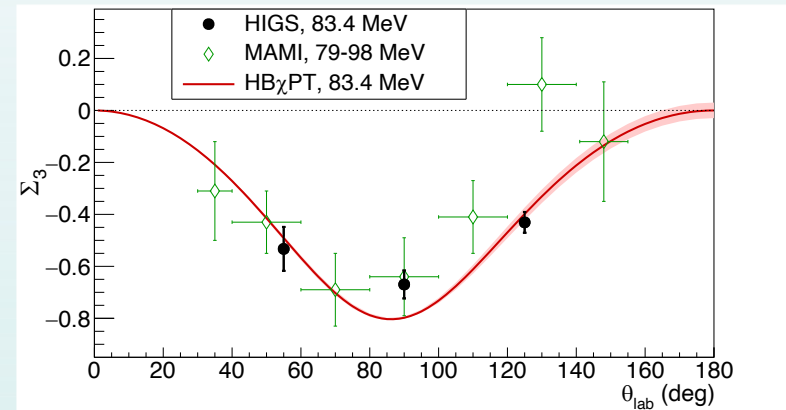
Proton Compton scattering results at HIγS

X. Li *et al.*, Phys. Rev. Lett. 128, 132502 (2022)

- **Polarized differential cross sections measured for the first time**
- **Provided a novel experimental approach to extract α_p and β_p**



$$\Sigma_3 = \frac{\sigma_\parallel - \sigma_\perp}{\sigma_\parallel + \sigma_\perp}$$



*HIGS Σ_3 values were calculated from polarized cross-section data

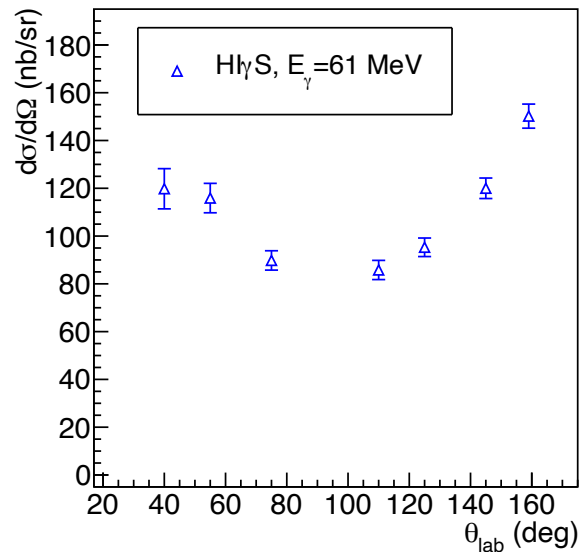
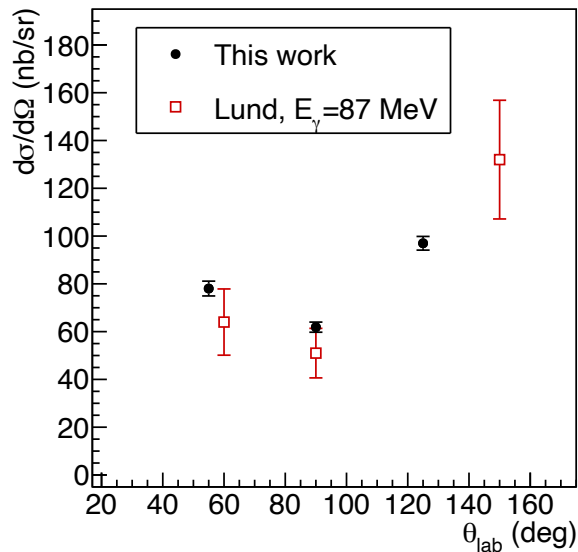
$$\sigma_{pol} = \sigma_{unpol}(1 \pm \delta_l \Sigma_3 \cos 2\phi)$$

V. Olmos de León *et al.*, Eur. Phys. J. A 10, 207 (2001)

B. E. MacGibbon *et al.*, Phys. Rev. C 52, 2097 (1995)

V. Sokhoyan *et al.* (A2 Collaboration), Eur. Phys. J. A 53, 14 (2017) 33

Elastic Compton scattering from ^4He at HI γ S



- **Fore-aft asymmetry** indicates a strong sensitivity to sub-nuclear effects
- α and β for the **neutron** can be extracted from the high precision ^4He data from HI γ S with future χEFT calculation

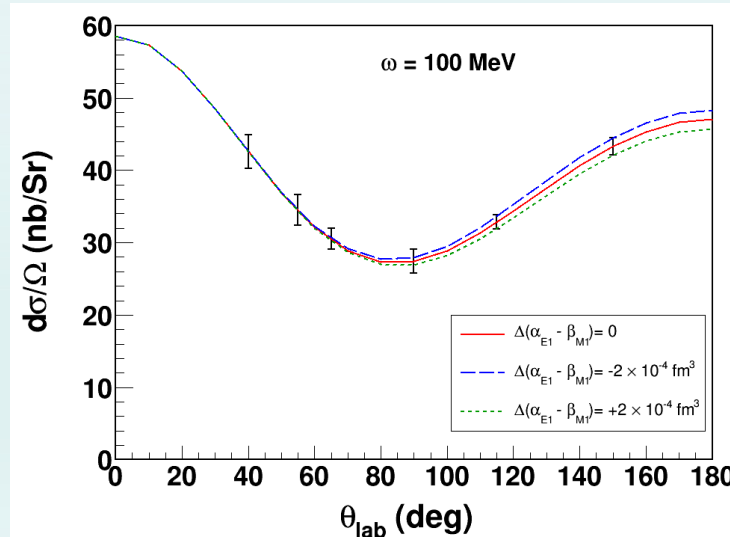
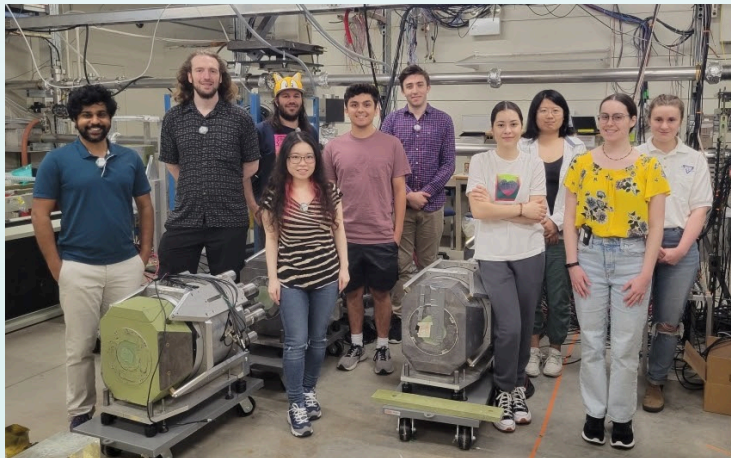
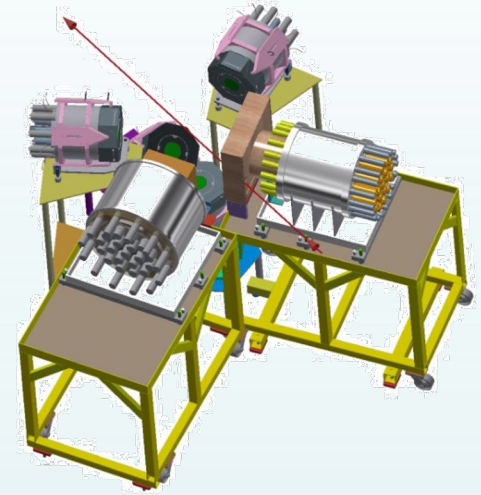
K. Fuhrberg *et al.*, Nucl. Phys. A **591**, 1 (1995) M. H. Sikora *et al.*, Phys. Rev. C **96**, 055209 (2017)

X. Li *et al.*, Phys. Rev. C **101, 034618 (2020)**

Compton scattering from ${}^3\text{He}$ at HIγS

The **first measurement** on ${}^3\text{He}$:

- Previously limited by the cryogenic technique
- The cross section is sensitive to the neutron polarizabilities
- $\sigma \sim Z$: $\sigma_{{}^3\text{He}} \sim 2\sigma_d$
- Higher **binding energy** than deuteron, less stringent requirement for the detector resolution
- The coherent cross section arises from a **different linear combination** of the nucleon contributions, another test case for the EFT formalism



Expected uncertainties of α_{E1}^n and β_{M1}^n

$$0.75 \times 10^{-4} \text{ fm}^3$$

Data taking
Spring 2024

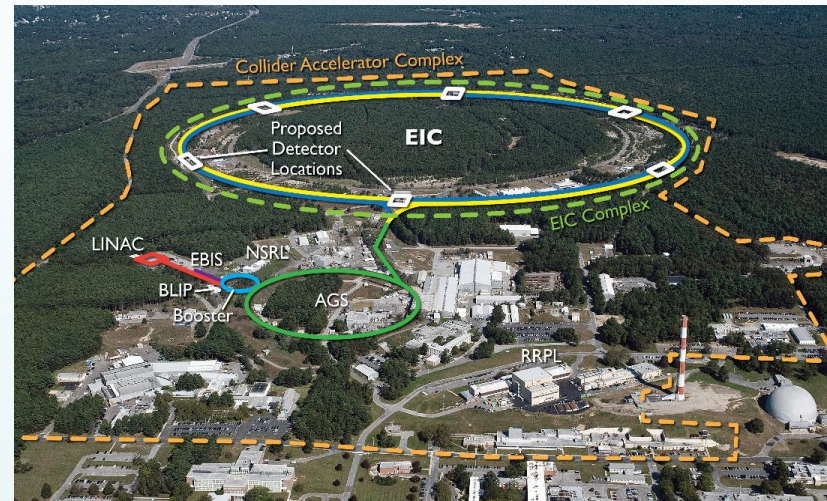
The Electron-Ion Collider

2015 NSAC LRP

“We recommend a high-energy high-luminosity polarized EIC as the highest priority for new facility construction following the completion of FRIB.”

- **Project Design Goals**

- High Luminosity: $L = 10^{33} - 10^{34} \text{cm}^{-2}\text{sec}^{-1}$, 10–100 fb⁻¹/year
 - Highly Polarized Beams: ~70%
 - Large Center of Mass Energy Range: $E_{\text{cm}} = 20 - 140 \text{ GeV}$
 - Large Ion Species Range: protons – Uranium
 - Large Detector Acceptance and Good Background Conditions
 - Accommodate a Second Interaction Region (IR)
-
- Conceptual design scope and expected performance meet or exceed NSAC Long Range Plan (2015) and the EIC White Paper requirements endorsed by NAS (2018)



Double Ring Design Based on Existing RHIC Facility



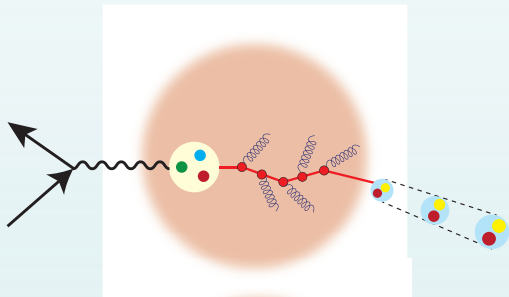
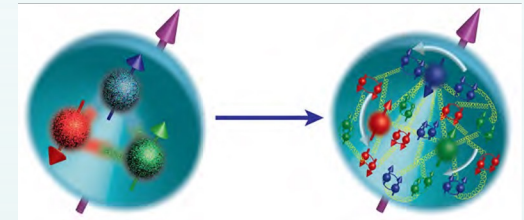
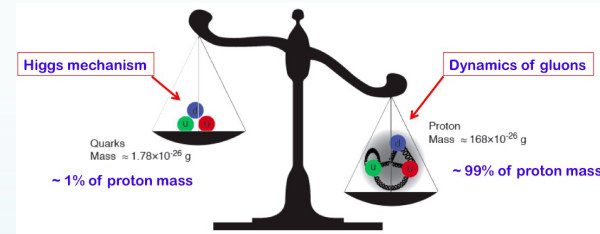
1391 collaborators, 37 countries, 276 institutions

NSAC Long Range Plan (2023) expected to endorse EIC.

EIC Physics at-a-Glance

How are the sea quarks and gluons, and their spins, **distributed in space and momentum** inside the nucleon?

How do the **nucleon properties (mass & spin)** emerge from their interactions?



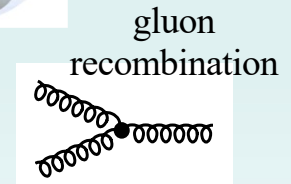
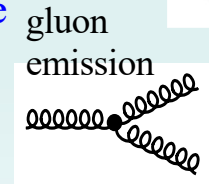
How do color-charged quarks and gluons, and colorless jets, **interact with a nuclear medium**?

How do the **confined hadronic states** emerge from these quarks and gluons?

How do the quark-gluon **interactions create nuclear binding**?

How does a **dense nuclear environment** affect the quarks and gluons, their correlations, and their interactions?

What happens to the **gluon density in nuclei**? Does it **saturate at high energy**, giving rise to a **gluonic matter with universal properties** in all nuclei, even the proton?





- **Acknowledgement: The PRad Collaboration, J. Bernauer, R. Gilman, S. Paul, T. Suda, W. Xiong, J. Zhou, S. Strauch, H. Merkel, M. Vanderhaeghen, and others; HIGS Compton Collaboration**
- **Supported in part by NSF MRI PHY-1229153 and the U.S. Department of Energy under contract number DE-FG02-03ER41231**